Angewandte Chemie
Eine Zeitschrift der Gesellschaft Deutscher Chemiker

Supporting Information

A Robust Porous Quinoline Cage: Transformation of a [4+6] Salicylimine Cage by Povarov Cyclization

*Pierre-Emmanuel Alexandre, Wen-Shan Zhang, Frank Rominger, Sven M. Elbert, Rasmus R. Schröder, and Michael Mastalerz**

anie_202007048_sm_miscellaneous_information.pdf

-Supporting Information-

Table of Contents

1. General Remarks

Reagents and Solvents: All reagents and solvents were obtained from abcr, Acros Organics, Carbolution, Sigma-Aldrich or VWR used without further purification unless otherwise stated. 4-(tert-butyl)-2,6-bis((E)-(p-tolylimino)methyl)phenol **S1** was synthesized according to the procedure reported in literature.[S1] [4+6]-Imine-Cage compound **1** was synthesized according to the procedure reported in literature.[S2]

Nuclear Magnetic Resonance Spectroscopy (NMR): NMR spectra (^{1}H, ^{13}C and 2D coupling experiments) were recorded on a Bruker Avance III 300 (^{1}H: 300 MHz; ^{13}C: 75 MHz), Bruker Avance III 400 (^{1}H: 400 MHz; ^{13}C: 100 MHz), Bruker Avance III 500 (^{1}H: 500 MHz; ^{13}C: 100 MHz) and a Bruker Avance III 600 (^{1}H: 600 MHz ^{13}C: 150 MHz) spectrometer at 298 K, unless otherwise mentioned. NMR spectra were internally referenced to residual solvent peaks in $CDCl_3$ (^{1}H-NMR: δ = 7.26 ppm, ^{13}C-NMR: 77.1 ppm), C_2DCl_2 (^{1}H-NMR: δ = 5.30 ppm), or in DMSO-d_6 (^{1}H-NMR: δ = 2.50 ppm, ^{13}C-NMR: 39.5 ppm). The evaluation of the spectra was carried out with help of the software MestReNova. Chemical shifts are reported as δ values (ppm) relative to the solvent peak and coupling constants (J) are given in Hz. Splitting patterns are designated as s, singlet, d, doublet, dd, doublet of doublet, m, multiplet, br, broad.

Diffusion Ordered Spectroscopy (DOSY): DOSY-NMR spectrum was recorded at 298 K and 400 MHz. Calibration was performed using the self-diffusion of the solvent (chloroform; D_{solv} =2.45·10^{-9}m^2.s^{-1}).[S3] The solvodynamic radii r_s of the cage compounds were calculated from the measured diffusion coefficients D using the semi-empirical modification of the Stokes-Einstein equation.[S4] This equation was solved numerically for r_s using literature know values for the solvodynamic radius r_{solv} and the viscosity η of the solvent (r_{solv} = 0.260 nm and η = 0.542·10^{-3} kg.ms^{-1} for chloroform at temperature T = 298K). [S5]

Equation S1:
$$D = \frac{\frac{k_B T}{6\pi\eta r_S}}{1+0.695\left(\frac{r_{solv}}{r_S}\right)^{2.234}}$$

Mass Spectroscopy (MS): MALDI-TOF mass spectra were measured by the MS service on a Bruker Daltonik Reflex III, on a Bruker ApexQe or on a Bruker AutoFlex Speed TOF with DCBT (trans-2-[3-(4-tertbutylphenyl)-2-methyl-2-propenylidene]malononitrile) as co-crystallizer for the matrix. HRMS experiments were carried out on a Fourier Transform Ion Cyclotron Resonance (FTICR) mass spectrometer solariX (Bruker Daltonik GmbH, Bremen,

Germany) equipped with a 7.0 T superconducting magnet and interfaced to an Apollo II Dual ESI/MALDI source.

Melting points (Mp.): The non-corrected melting points were determined with a Büchi Melting Point B-545.

Ultraviolet-Visible and Fluorescence Spectroscopy: Absorption spectra were measured on a JASCO UV-VIS V-730 machine. Absorption-spectra scans were recorded in DCM, at room temperature between 600 nm and 250 nm (0.5 nm resolution). Absorption-spectra scans were recorded in DMSO at 40 °C, between 600 mn and 270 nm (0.5 nm resolution). Emission spectra were measured on a JASCO FP-9300 machine. Emission-spectra scans were recorded in at room temperature except for DMSO at 40 °C between 350 nm and 700 nm (0.5 nm resolution). Quantum yields Φ were obtained by the absolute method[S6] using a PTI Quantum Master 40 with an Ulbricht integration sphere (LabSphere®, diameter:6", coated with Spectraflect®). The reported quantum yields Φ are average values of three independents measurements.

Infrared Spectroscopy (IR): IR-Spectra were recorded on a Bruker Lumos spectrometer equipped with a Ge ATR crystal. The signal intensity was described with: s (strong), m (medium), w (weak) and br (broad).

Thermal Gravimetric Analysis (TGA): Thermal gravimetric analyses were measured on a Mettler-Toledo TGA/DSC1 instrument with a TGA/DSC-Sensor 1100 equipped with a MX1 balance (Mettler-Toledo) and a GC100 gas control box for nitrogen supply. TGA samples were measured in 70 HL Al_2O_3 crucibles. All measurements were carried out under flow of nitrogen (10 $mL.min^{-1}$).

Powder Diffraction (PXRD): Powder diffractometry was performed with a STOE STADI 611KLS/N 61263 with Ge (111) - monochromatic copper radiation (λ (CuKα) = 1.54060 Å). The diffractograms were obtained with a Stoe linear PSD Detector, measured in a glass capillary (Ø = 0.7 mm) as sample container.

Gassorption Experiments: The surface area and porosity were characterized by nitrogen adsorption and desorption analysis at 77.35 K with an autosorb computer-controlled surface analyzer (AUTOSORB-iQ, Quantachrome). The Brunauer-Emmett-Teller (BET) surface areas were calculated assuming a cross sectional area of 0.162 nm^2 for the nitrogen molecules in the pressure range P/P_0 = 0.01-0.1. Pressure range that have a positive slope in the Rouquerol

plot were considered. Uptake measurement of H_2 was done at 77 K and of CH_4 and CO_2 at 273 K, carried out using a simple Dewar vacuum flask with an ice/water mixture. A frozen mixture of water/ethanol (80:20, v/v) was used for the measurements at 263 K. The temperatures were controlled with a VWR TD 131 digital thermometer.

Scanning Electron Microscopy (SEM): Electron micrographs were acquired by using a Crossbeam 540 field emission scanning electron microscope (Carl Zeiss Microscopy, Germany). Imaging was performed with a working distance of 3.0 mm and a landing energy between 1.0 keV and 3.0 keV. The secondary electron images were recorded by an Inlens-detector and the backscattered electron images recorded by an EsB-detector. The powder sample was suspended in isopropanol, treated with ultrasound and drop-casted onto a silicon wafer substrate pre-cleaned in air-plasma. Silicon water: single side polished p-type (100), from Si-Mat, Germany

X-ray Crystal structure Analysis: Crystal structure analysis were accomplished on Bruker APEX II Quazar diffractometer with a molybdenum source (λ(Mo Kα= 0.71073 Å).

Thin Layer Chrommatography (TLC): Thin layer chromatography was performed with Merk KGaA Darmstadt Silica gel 60 F_{254} precoated silica gel sheets with visualization by ultraviolet light (254 nm and 366 nm)

Column Chromatography: Column chromatography was carried out with MACHEREY-NAGEL GmbH & Co. KG Silica 60 (0.04-0.63 mm).

2. Experimental Procedures

Synthesis of model compound 3.

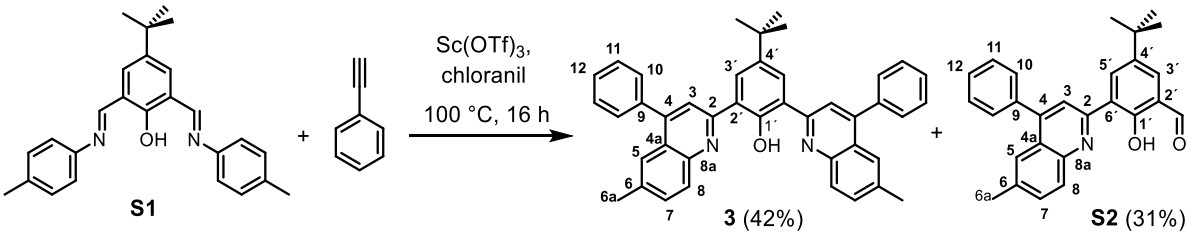

Salicylimine **S1** (155 mg, 0.40 mmol), scandium triflate (118 mg, 0.24 mmol) and chloranil (198 mg, 0.80 mmol) were suspended in phenylacetylene (1.3 mL, 30.0 eq.). The reaction mixture was stirred for 16 hours at 100 °C. After cooling the reaction mixture down to room temperature, it was diluted with CH_2Cl_2 (50 mL) and the organic phase washed with $NaHCO_3$ sat. solution (2x 50 mL), water (50 mL), and brine (50 mL) and dried over $MgSO_4$. Solvent was removed by rotary evaporation and the crude product was purified via column chromatography (PE/EE, 40/1 to 10/1, *v/v*) to give as first fraction (R_f = 0.21) 60 mg (31%) of quinoline **3** as an orange solid. Mp. 175 °C. ^{1}H NMR (300 MHz, $CDCl_3$) δ = 16.30 ppm (s, 1H, -*OH*), 10.69 (s, 1H, -*CH*=O), 8.19 (d, 2H, *J* = 2.5 Hz -*H5´*), 8.01 (m, 1H, -*H8*), 7.95 (d, 2H, *J* = 2.5 Hz -*H3´*), 7.91 (s, 1H, -*H3*), 7.65-7.55 (m, 7H, -*H5,7,10-12*), 2.49 (s, 6H, -C*H*$_3$), 1.38 (s, 9H, -C(C*H*$_3$)$_3$). ^{13}C NMR (75 MHz, $CDCl_3$): δ = 190.8 ppm (*C*=O), 162.6 (C-*1´*), 155.90 (C-*2*), 150.3 (C-*8a*), 143.4 (C-*4*), 141.1 (C-*4´*), 138.0 (C-*5´*), 137.6 (C-*6*), 133.1 (C-*7*), 130.4 (C-*3´*), 129.6 (C-*10,11*), 129.0 (C-*12*), 127.8 (C-*9*), 127.5 (C-*8*), 125.7 (C-*4a*), 124.9 (C-*5*), 124.5 (C-*2´*), 120.0 (C-*6´*), 117.6 (C-*3*), 34.5 (*C*-(CH$_3$)$_3$), 31.6 (C-(*CH*$_3$)$_3$), 22.0 (C-*6a*). IR (neat, ATR): $\tilde{\nu}$ = 2958.7 cm^{-1} (m), 1678.0 (vs), 1604.7 (m), 1589.3 (vs), 1552.6 (s), 1477.4 (s), 1462.0 (m), 1394.5 (m), 1361.7 (m), 1274.9 (m), 1251.7 (s), 1222.8 (m), 1130.2 (w), 1085.9 (m), 947.0 (m), 923.9 (m), 887.2 (m), 864.1 (m), 817.8 (m), 798.5 (w), 771.5 (m), 704.0 (vs), 624.9 (s). UV/Vis (DCM): λ_{max} (log ε) = 370 mn (4.15), 260 (4.60). HRMS (DART) *m/z* calculated for $C_{27}H_{26}N_2O[M+H]^+$: 396.196, found 396.195.calculated for $C_{84}H_{73}N_4O_2$ $[2M+H]^+$: 791,384, found 791,784. Elemental analysis (%) calculated for $C_{27}H_{25}NO_2 \cdot H_2O$: C 78.42, H 6.58, N 3.39; found C 79.76, H 6.89, N 3.17.

The second fraction (R_f = 0.18) gave 84 mg (35%) of **S2** as yellow solid. Mp. 236-237 °C. ^{1}H NMR (600 MHz, DMSO-d_6) δ = 16.06 ppm (s, 1H, -*OH*), 8.27 (s, 2H, -*H3*), 8.20 (s, 2H, -*H3´*), 8.10 (d, *J* = 8.5 Hz, 2H, -*H8*), 7.67-7.59 (m, 14H, -*H5,7,10-12*), 2.46 (s, 6H, -C*H*$_3$), 1.42 (s, 9H, -C(C*H*$_3$)$_3$). ^{13}C NMR (150 MHz, DMSO-d_6): δ = 156.5 ppm (C-*1´*), 156.0 (C-*2*), 147.8 (C-

8a), 144.7 (C-*4*), 140.65 (C-*4´*), 137.6 (C-*9*), 136.5 (C-*6*), 132.1 (C-*7*), 129.5 (C-*10*), 128.7 (C-*11*), 128.5 (C-*12*), 128.4 (C-*8*), 128.0 (C-*3´*), 124.8 (C-*4a*), 124.0 (C-*5*), 123.2 (C-*2´*), 120.9 (C-*3*), 34.3 (*C*-(CH_3)$_3$), 31.4 (C-(*CH_3*)$_3$), 21.4 (C-*C*H_3). IR (neat, ATR): $\tilde{\nu}$ = 2954.8 cm-1 (w), 2925.9 (w), 2856.4 (vw), 1624.0 (w), 1589.3 (m), 1550.7 (m), 1489.0 (m), 1463.9 (m), 1444.6 (m), 1409.9 (w), 1392.5 (w), 1375.2 (vw), 1361.7 (w), 1340.5 (w), 1317.3 (w), 1284.5 (m), 1255.6 (m), 1232.5 (w), 1207.4 (w), 1159.2 (w), 1134.1 (w), 1116.7 (w), 1072.4 (w), 1031.9 (w), 910.4 (w), 891.1 (m), 875.6 (m), 840.9 (w), 825.5 (m), 802.4 (w), 781.1 (m), 763.8 (m), 700.1 (vs), 657.7 (vw), 644.2 (w), 624.9 (m). UV/Vis (DCM): λ_{max} (log ε) = 364 mn (3.90), 268 (4.41). HRMS (ESI): *m/z* calculated for $C_{42}H_{37}N_2O$ $[M+H]^+$: 585.290, found 585.290; calculated for $C_{84}H_{73}N_4O_2$[2M+H]$^+$: 1169.573, found 1169.574. Elemental analysis (%) Calculated for $C_{42}H_{36}N_2O \cdot 1.5\ H_2O$: C 82.46, H 6.43, N 4.58; found C 82.57, H 5.98, N 4.51.

Synthesis of quinoline cage 2.

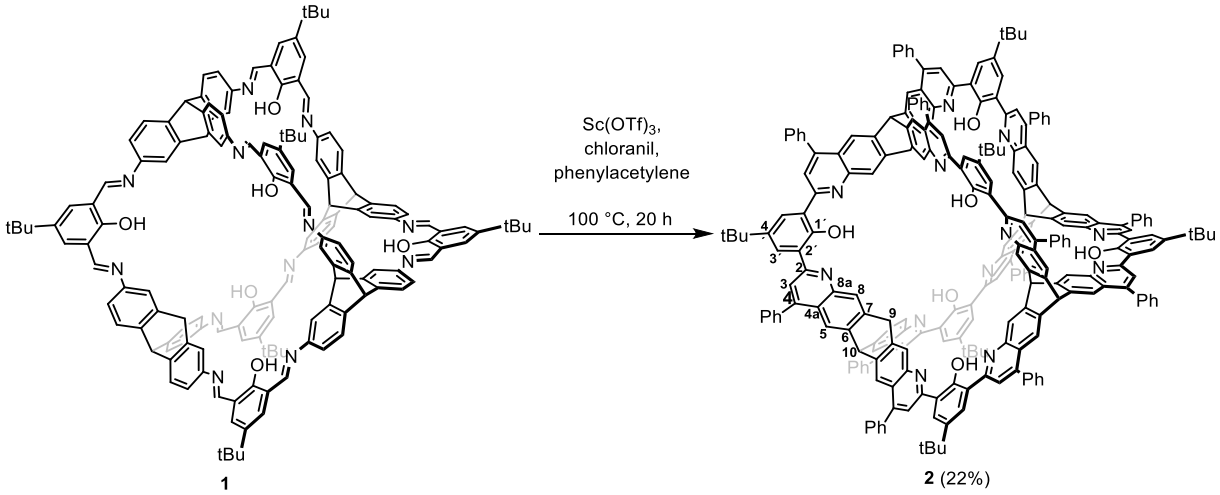

Imine cage **1** (100 mg, 0.05 mmol), $Sc(OTf)_3$ (79.8 mg, 0.16 mmol) and chloranil (132.9 mg, 0.54 mmol) were placed in a screw-cap vial (3 mL). Phenylacetylene (1.8 mL, 18.0 mmol, 360 eq.) was added and the reaction mixture was stirred for 20 hours at 100 °C. After collong down the reaction mixture to room temperature, dichloromethane (50 mL) was added and the organic phase washed with a sat. solution of $NaHCO_3$ (2 x 50 mL) and brine (50 mL), and dried over $MgSO_4$. After removal of solvents by rotary evaporation, the dark red oil was immersed with MeOH (10 mL) and solvent removed again to remove traces of phenylacetylene by co-evaporation. The remaining brown solid was dissolved in dichloromethane (2 mL) and precipitated by the addition of MeOH (25 mL). The solid was collected by filtration on a glas funnel and washed with MeOH (20 mL) and dried in air. Purification by column

chromatography (first column DCM 100% -> DCM/MeOH 0.5% to 5%; second column DCM/MeOH 2%). The collected fraction (R_f (CH_2Cl_2/MeOH = 100:4) = 0.23) was treated with MeOH (5 mL) and dried overnight at the Kugelrohr oven (250 °C $1.0 \cdot 10^{-3}$ mbar) to give 38 mg (22%) of quinoline cage **2** as a pale-orange solid. Mp. > 400 °C. ^{1}H NMR (600 MHz, $CDCl_3$ + 0.1 mol% triethyl-d_{15}-amine): δ =14.70 ppm (s, 6H, -O*H*), 8.62 (s, 12H, H*8*), 7.83 (s, 12H, -H*5*), 7.67 (s, 12H, H*3´*), 7.66 (s, 12H, H*3*), 7.54-7.60 (m, 60H, phenyl-H), 6.31 (s, 4H, -H*9*), 5.54 (s, 4H, -H*10*), 1.30 (s, 54H, -C(CH_3)$_3$). ^{13}C NMR (150 MHz, $CDCl_3$ + 0.1 mol% triethyl-d_{15}-amine): δ = 158.1 ppm (C-*1´*), 156,1 (C-*2*), 149.0 (C-*4*), 146.5 (C-*8a*), 144.7 (C-*7*), 141.3 (C-*6*), 141.1 (C-*4´*), 138.8 (*phenyl*-C), 129.8 (*phenyl*-C), 129.1 (C-*3´*), 128.8 (*phenyl*-C), 128.5 (*phenyl*-C), 124.7 (C-*2´*) 124.6 (C-*8*), 124.1 (C-*4a*), 120.9 (C-*3*), 119.9 (C-*5*), 53.5 (C-*9*), 53.5 (C-*10*), 34.3 (*C*-(CH_3)$_3$), 31.6 (C-(*C*H_3)$_3$). IR (neat, ATR): $\tilde{\nu}$ = 3372 cm-1 (w), 3058 (w), 3030 (w), 2958 (m), 2906 (w), 2886 (w), 1683 (w), 1587 (s), 1550 (s), 1483 (s), 1463 (s), 1444 (s), 1407 (m), 1363 (s), 1348 (m), 1271 (s), 1251 (s), 1168 (m), 1128 (m), 1074 (w), 1028 (w), 1001 (w), 896 (m), 877 (s), 840 (w), 825 (m), 765 (s), 700 (s), 646 (w), 615 (m). UV/Vis (DCM): λ_{max} (logε) = 354 nm (5.42), 264 (5.80). HRMS MALDI (DCBT) $[M]^+$: calculated for $C_{248}H_{176}N_{12}O_6$, 3417.383, found 3417.380. $[M+H]^+$: calculated for $C_{248}H_{177}N_{12}O_6$, 3418.390, found 3418.387.

3. Spectra

3.1 ^{1}H and ^{13}C NMR Spectra

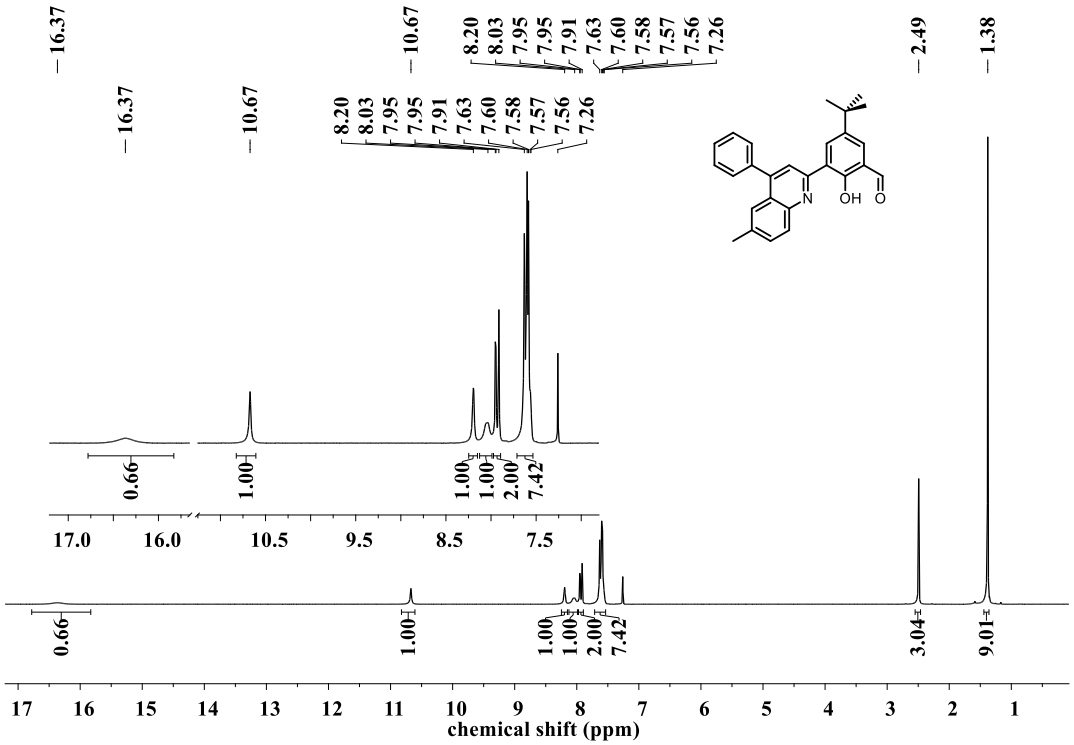

Figure S1. ^{1}H NMR (300 MHz, $CDCl_3$) spectrum of compound **S2**.

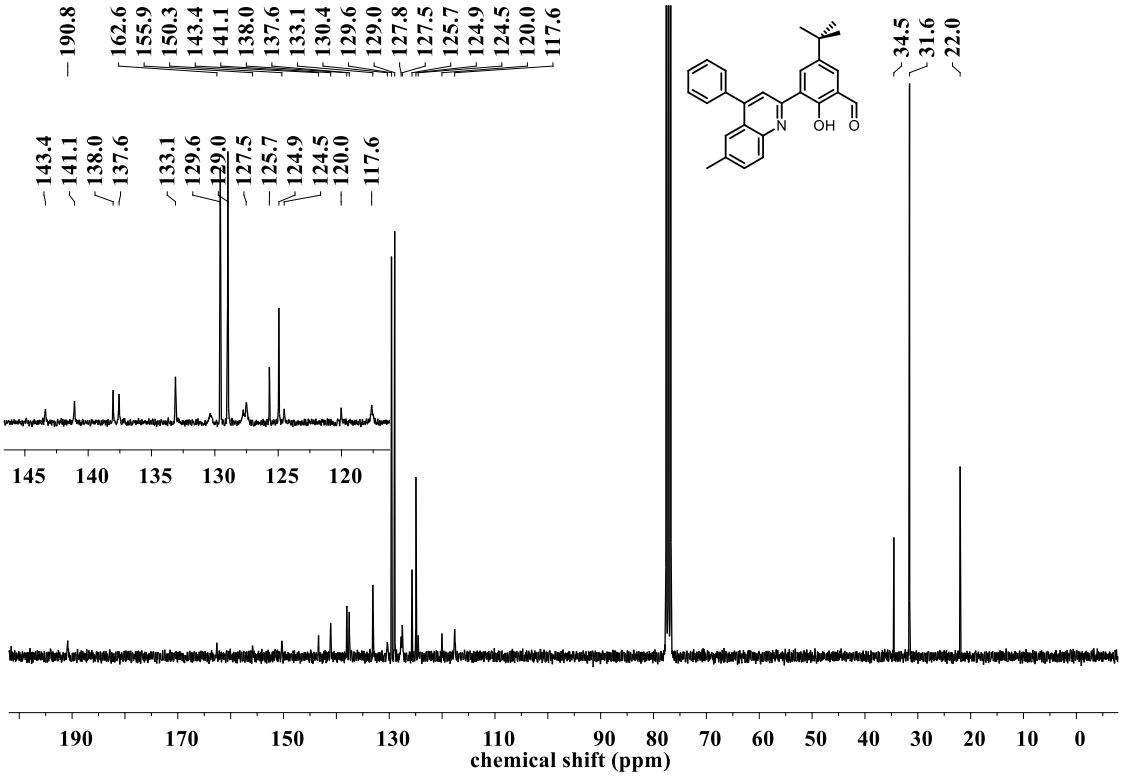

Figure S2. ^{13}C NMR (75 MHz, $CDCl_3$) spectrum of compound **S2**.

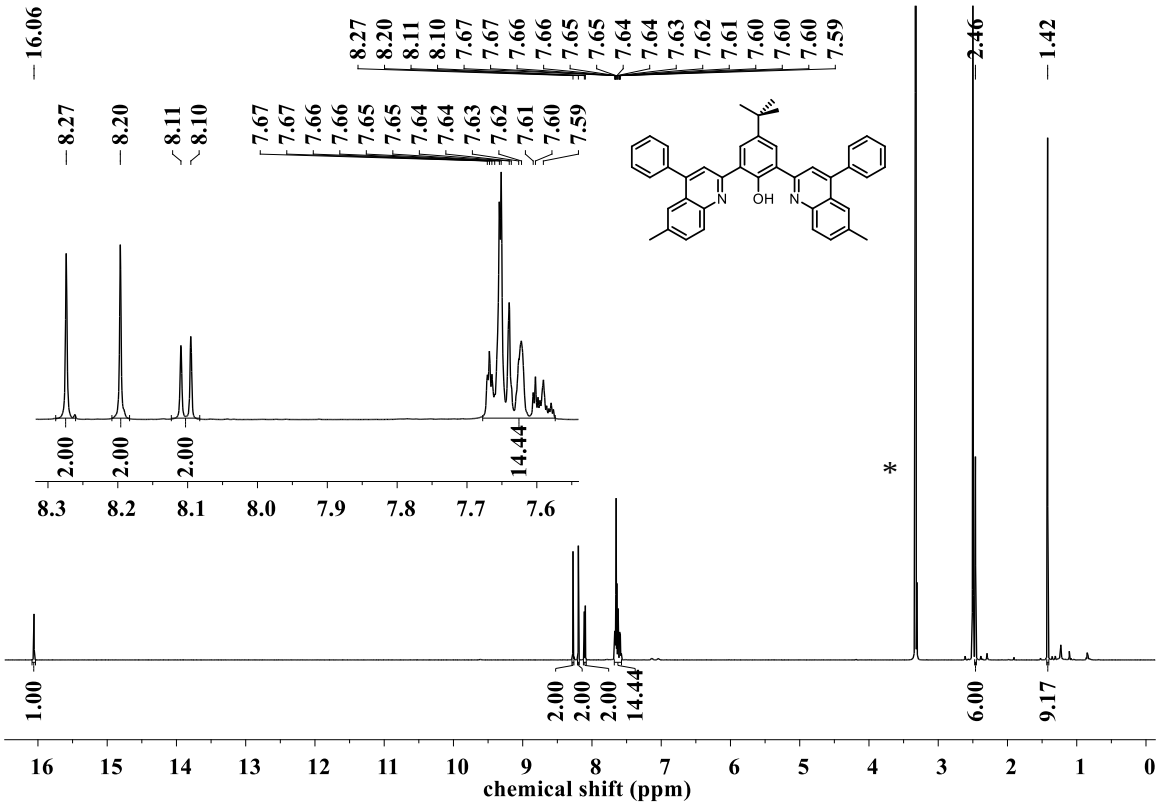

Figure S3. ^{1}H NMR (600 MHz, DMSO-d_6) spectrum of model compound **3**, * H_2O.

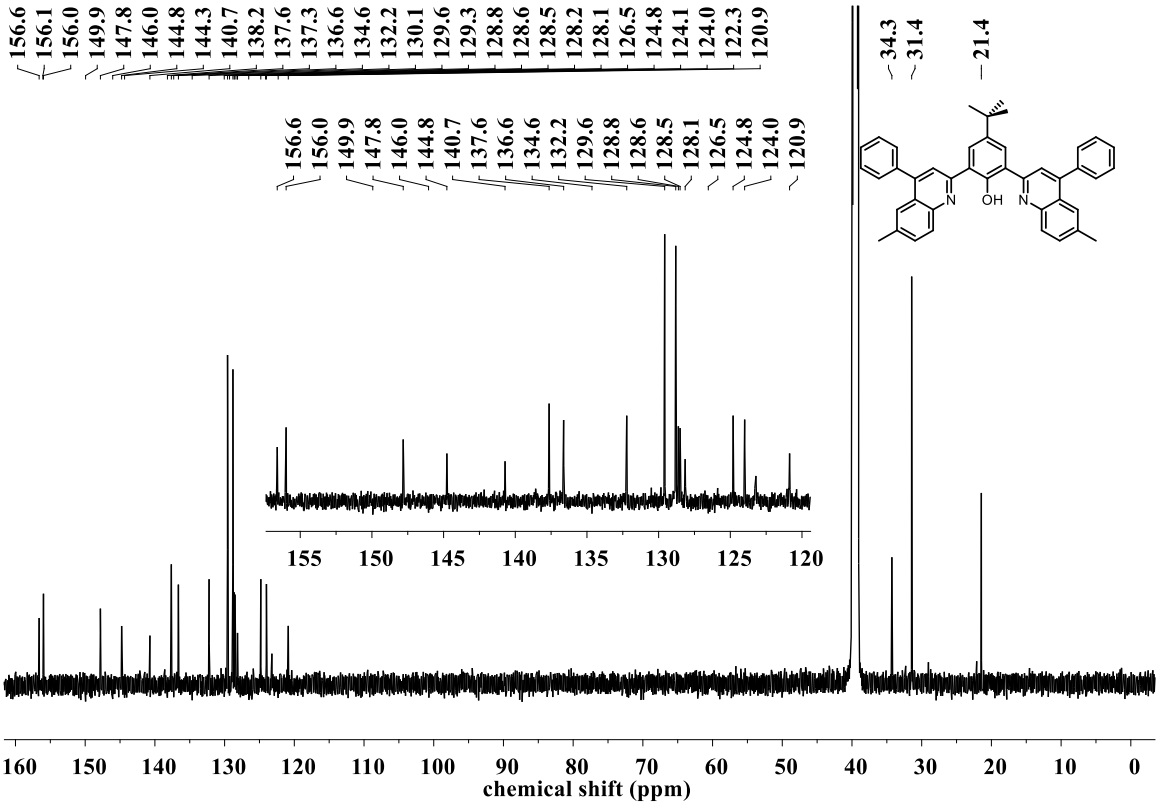

Figure S4. ^{13}C NMR (150 MHz, DMSO-d_6) spectrum of model compound **3**.

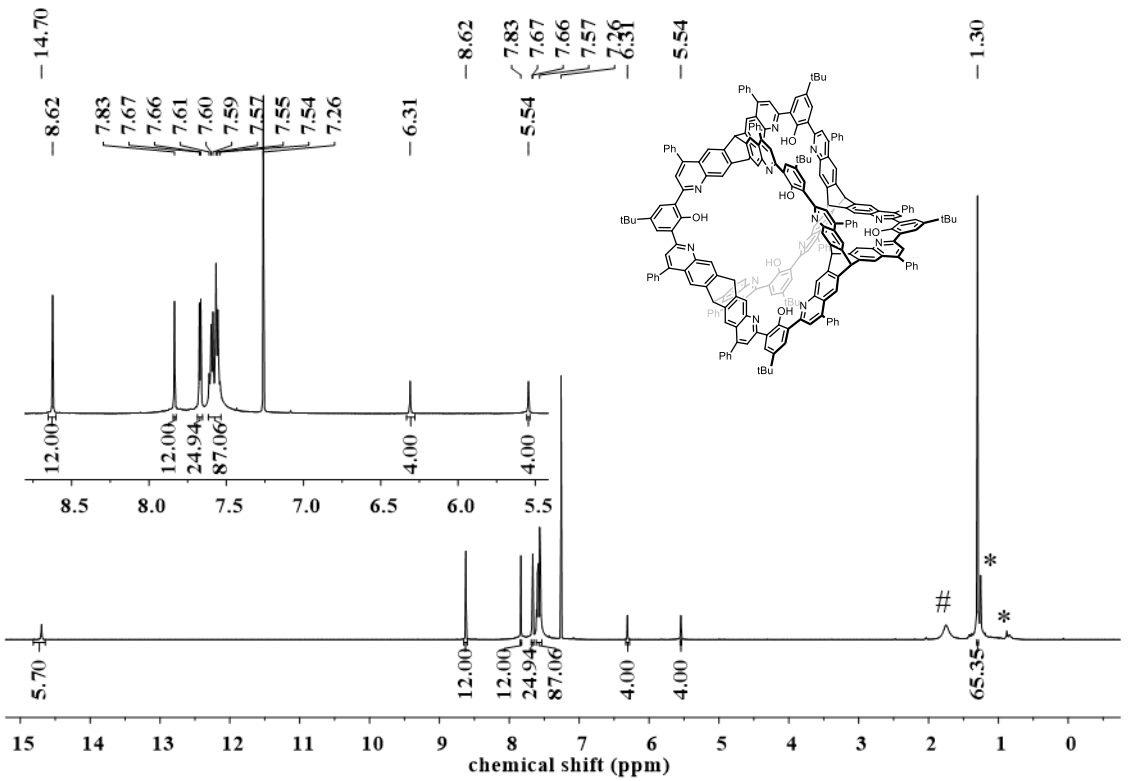

Figure S5. ^{1}H NMR (600 MHz, $CDCl_3$ +0.1 mol% triethyl-d_{15}-amine) spectrum of cage compound **2**. * n-hexane, # H_2O.

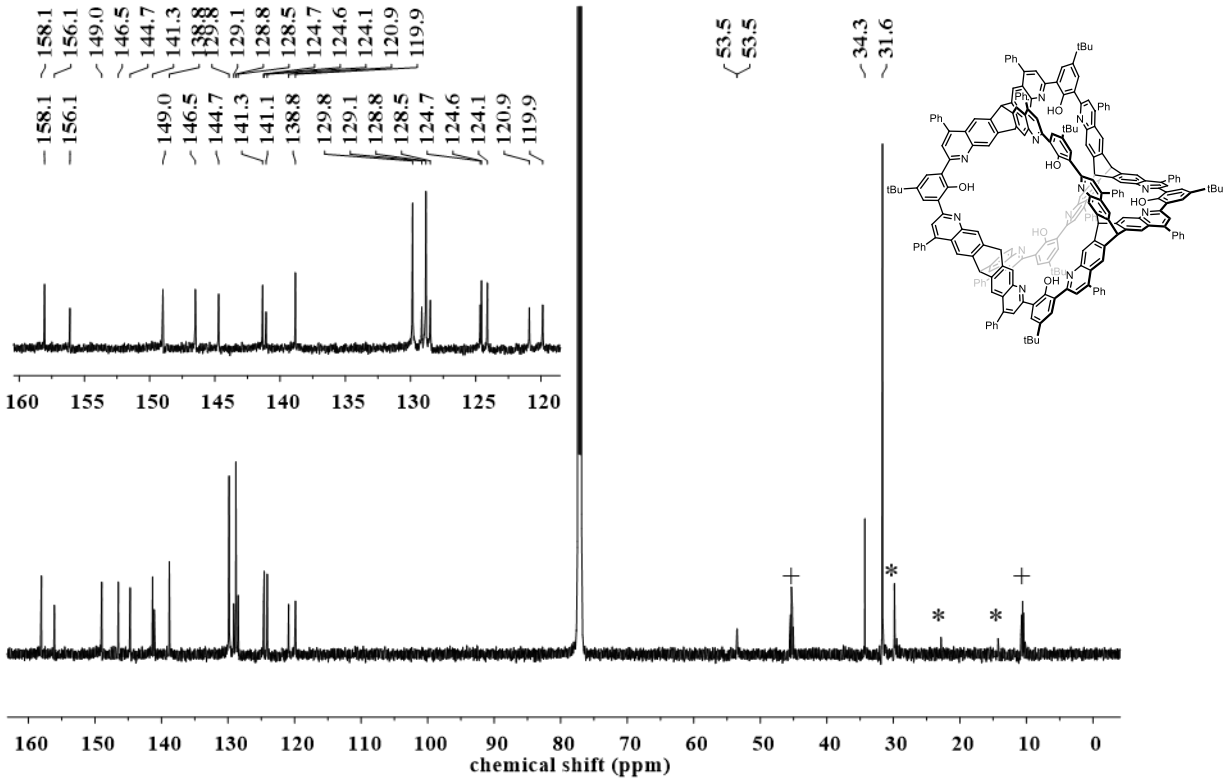

Figure S6. ^{13}C NMR (150 MHz, $CDCl_3$ + 0.1 mol% triethyl-d_{15}-amine, +) spectrum of cage compound **2**.* n-hexane.

3.2 2D-NMR spectra

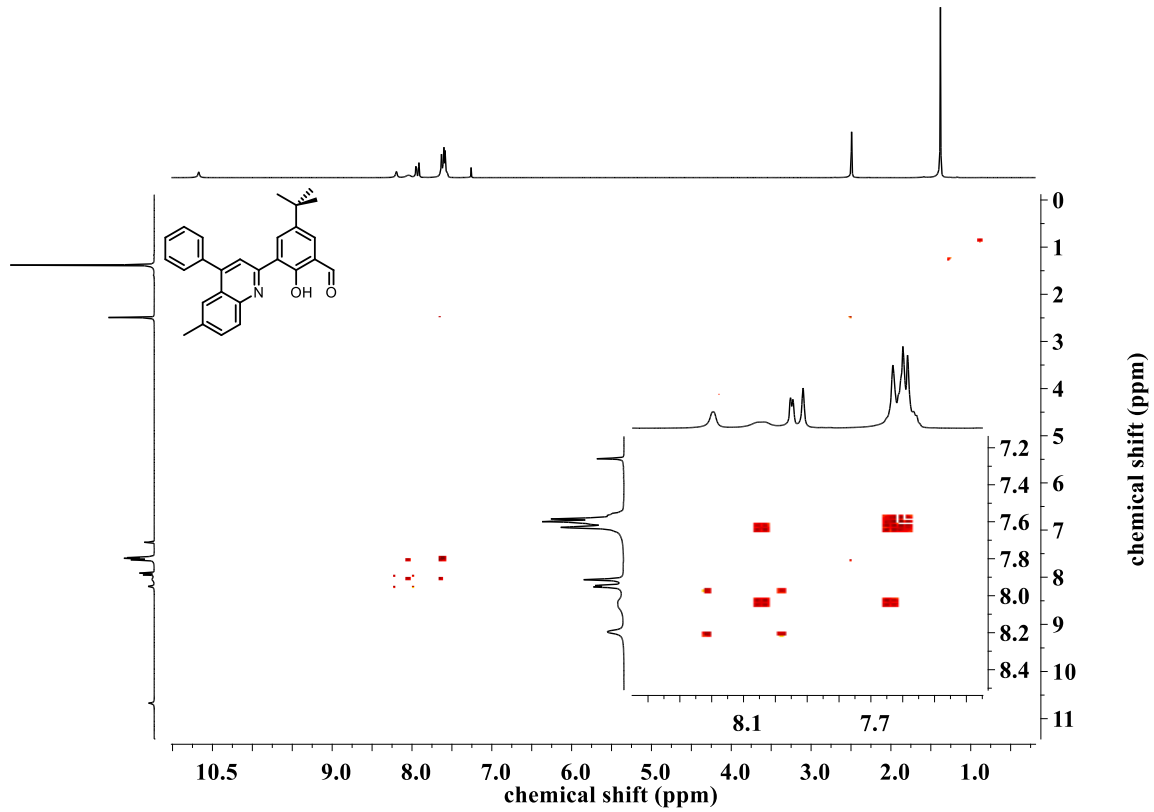

Figure S7. ^{1}H-^{1}H-COSY NMR (300 MHz, $CDCl_3$) spectrum of compound **S2**.

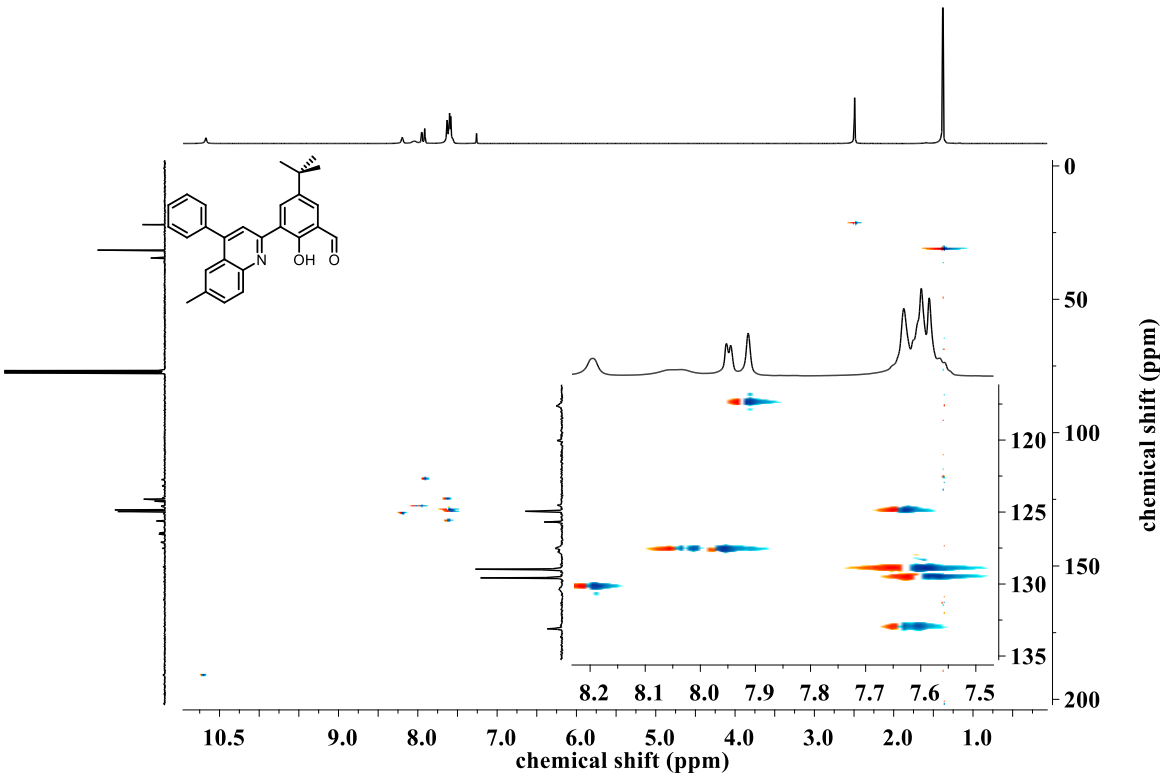

Figure S8. ^{1}H-^{13}C-HSQC NMR (300/75 MHz, $CDCl_3$) spectrum of compound **S2**.

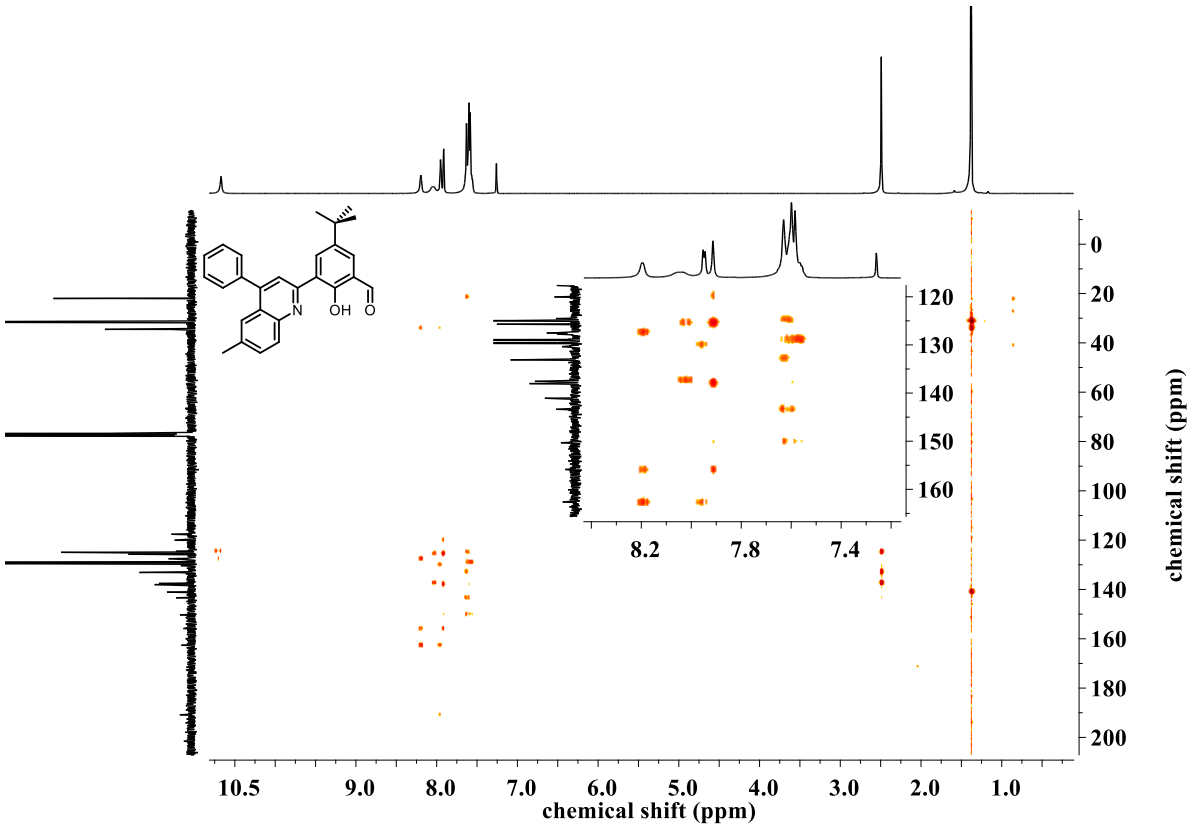

Figure S9. ^{1}H-^{13}C-HMBC NMR (300/75 MHz, $CDCl_3$) spectrum of compound **S2**.

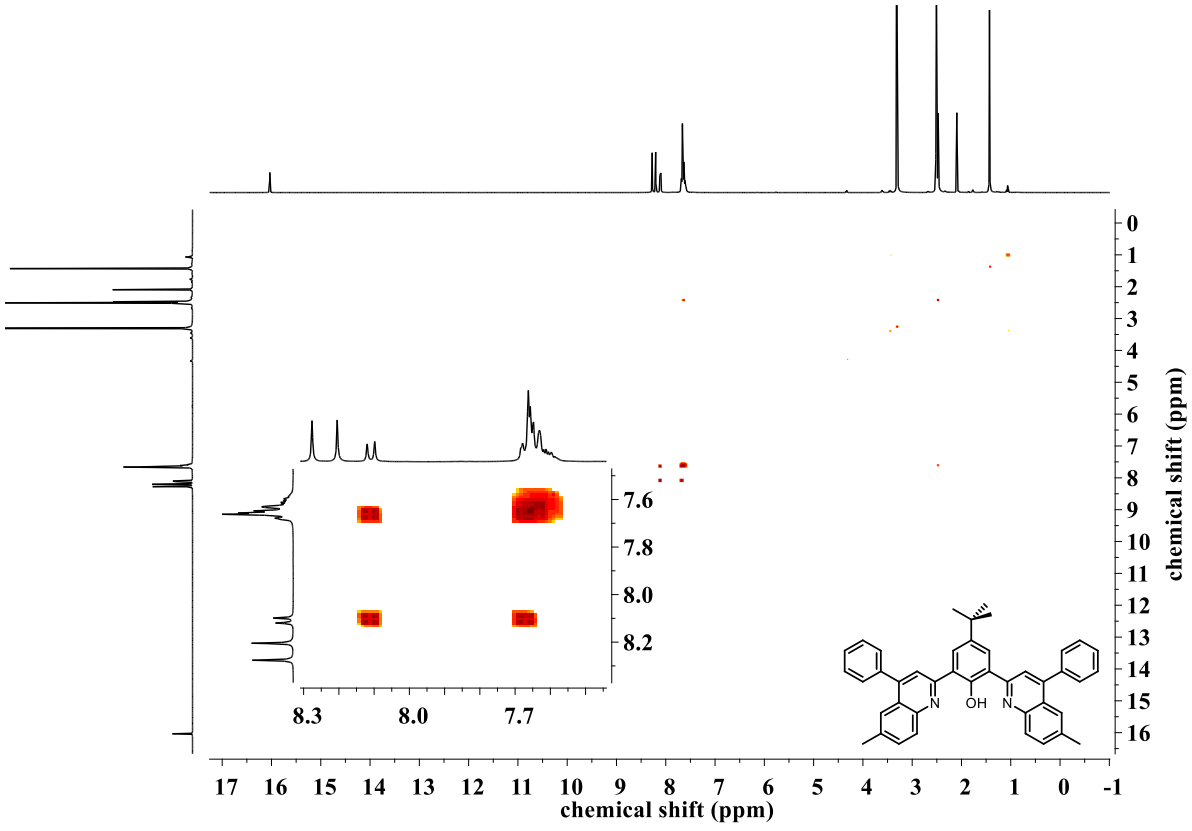

Figure S10. ^{1}H-^{1}H-COSY NMR (400 MHz, DMSO-d_6) spectrum of model compound **3**.

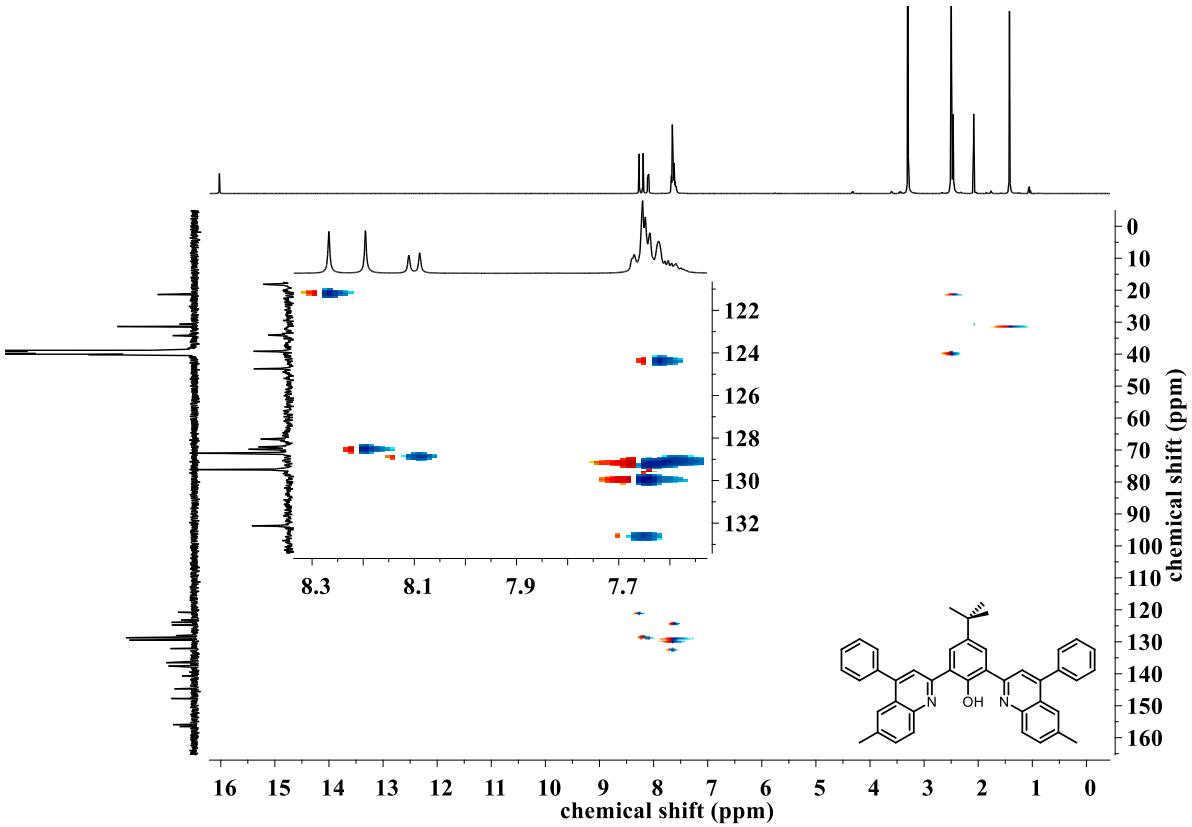

Figure S11. ^{1}H-^{13}C-HSQC NMR (400/100 MHz, DMSO-d_6) spectrum of model compound **3**.

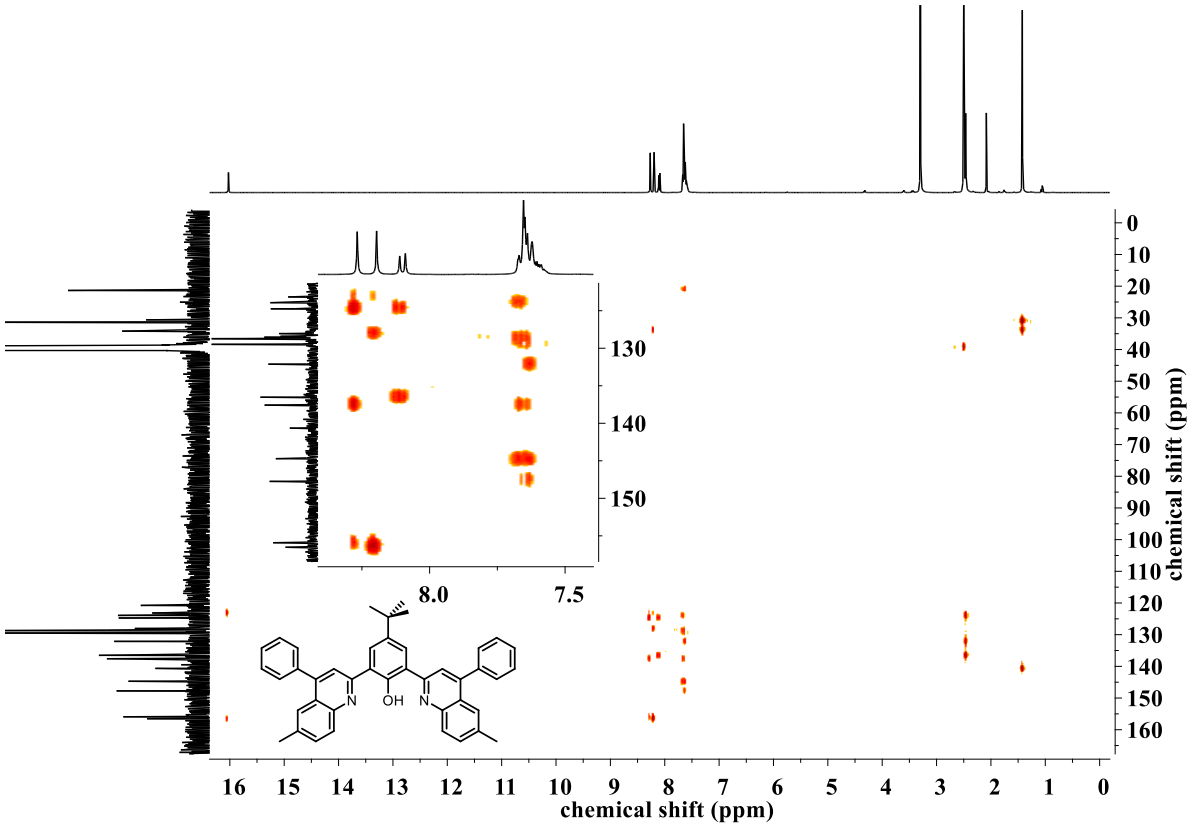

Figure S12. ^{1}H-^{13}C-HMBC NMR (400/100 MHz, DMSO-d_6) spectrum of model compound **3**.

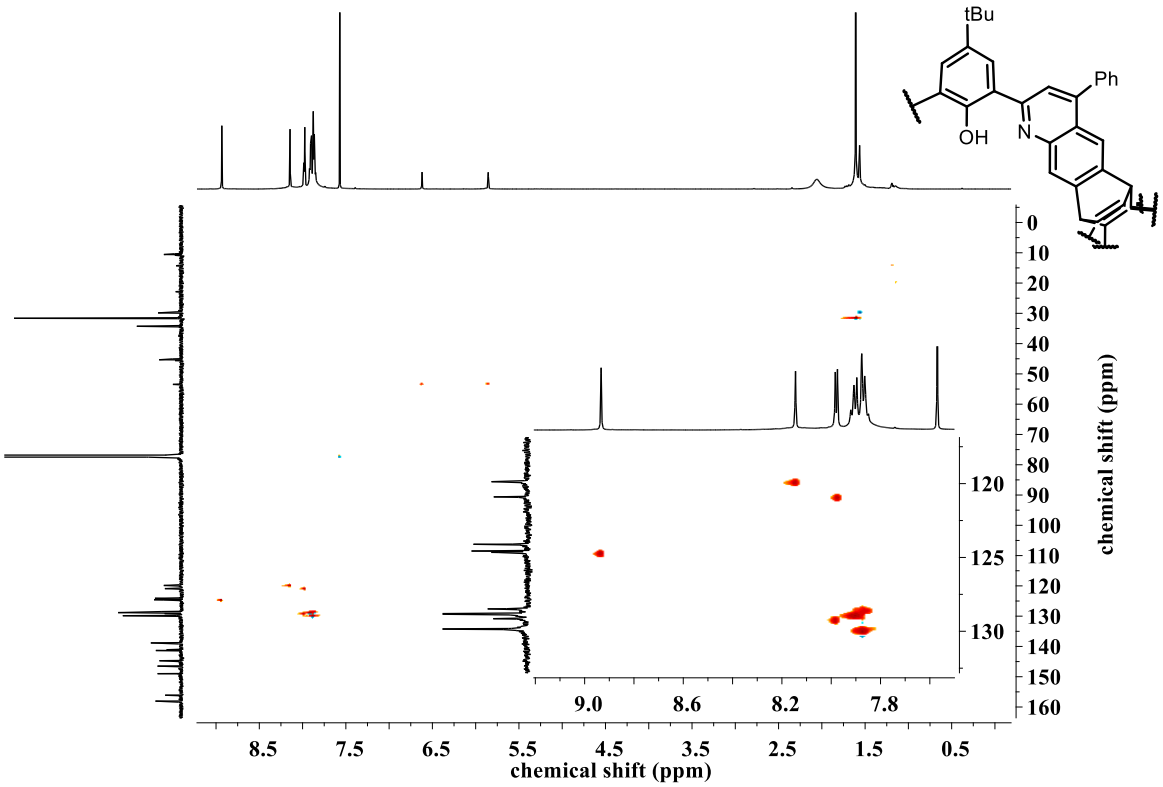

Figure S13. ^{1}H-^{13}C-HSQC (600/150 MHz, $CDCl_3$ + 0.1 mol% triethyl-d_{15}-amine) spectrum of cage compound **2**.

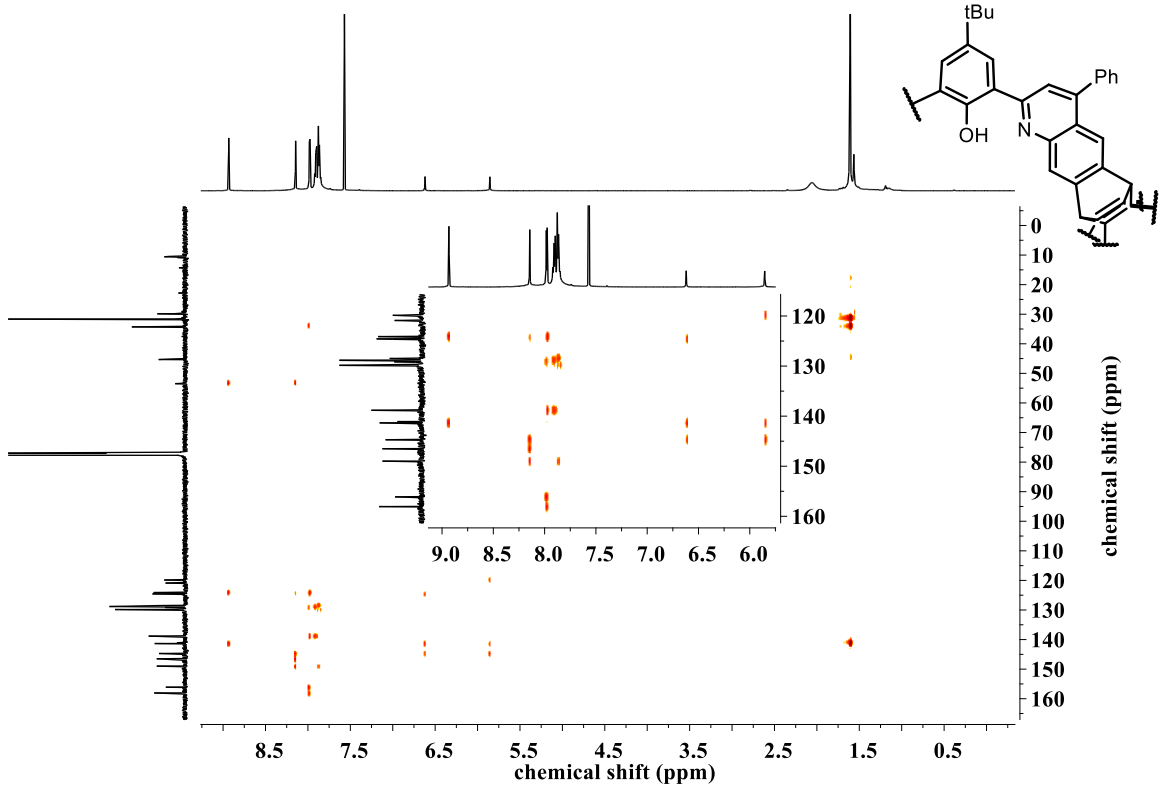

Figure S14. ^{1}H-^{13}C-HMBC (60/-150 MHz, $CDCl_3$ + 0.1 mol% triethyl-d_{15}-amine) spectrum of cage **2**.

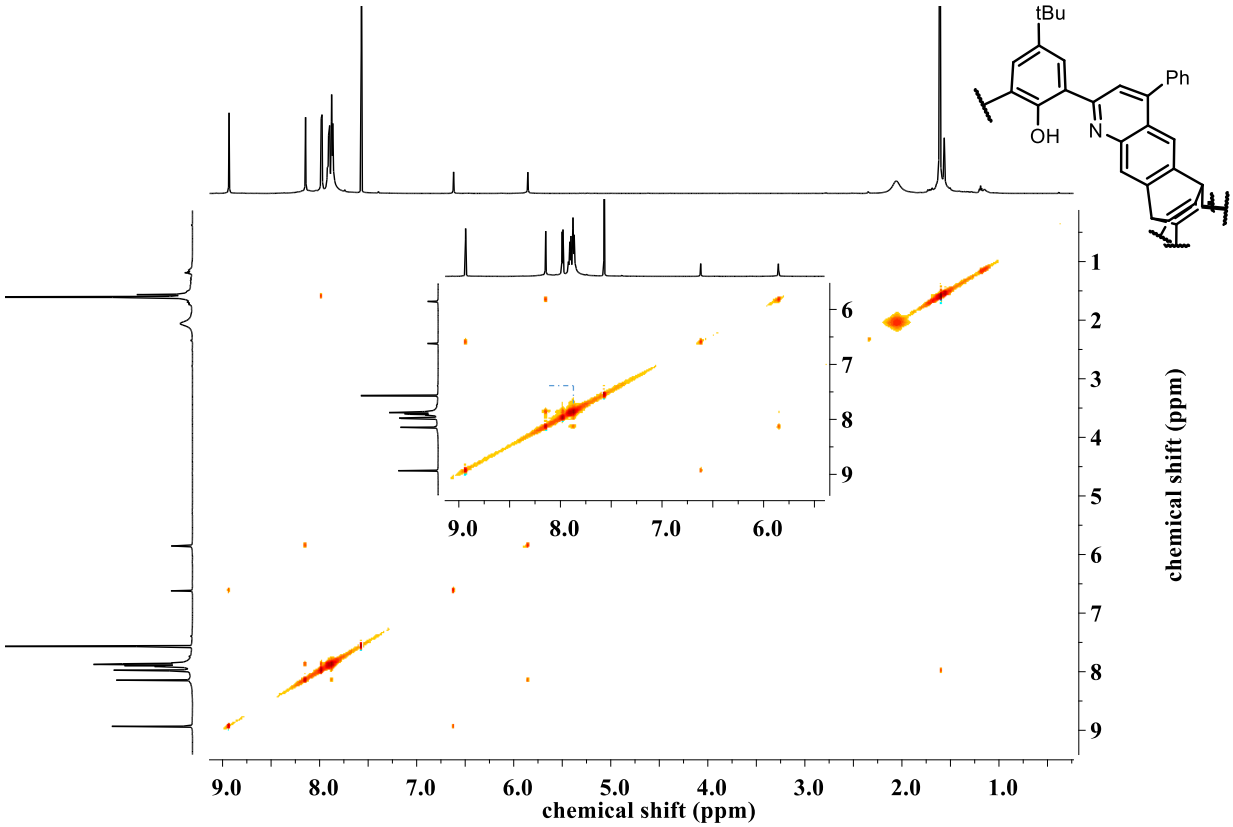

Figure S15. ^{1}H-^{1}H -NOESY (600 MHz, $CDCl_3$ + 0.1 mol% triethyl-d_{15}-amine) spectrum of cage **2**.

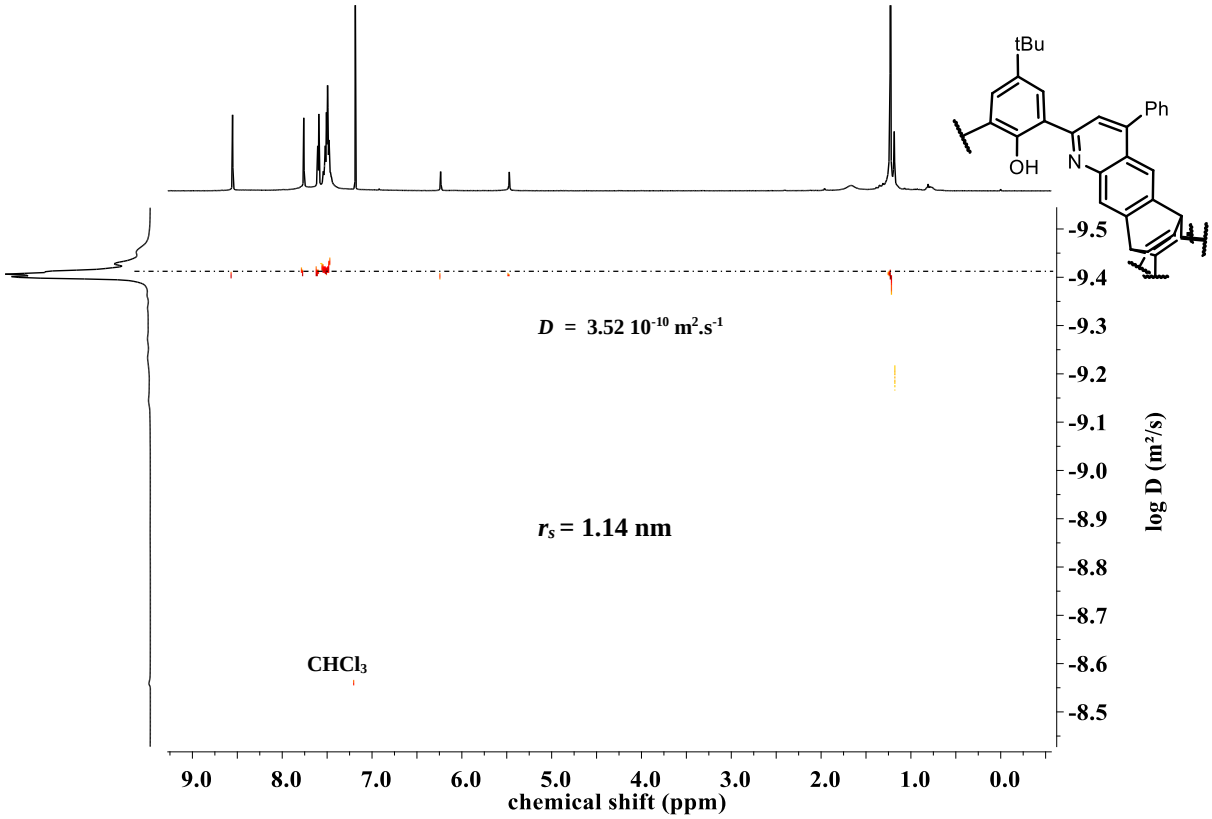

Figure S16. ^{1}H-DOSY (400 MHz, $CDCl_3$ + 0.1 mol% triethyl-d_{15}-amine) spectrum of cage **2**.

3.3 Mass Spectra

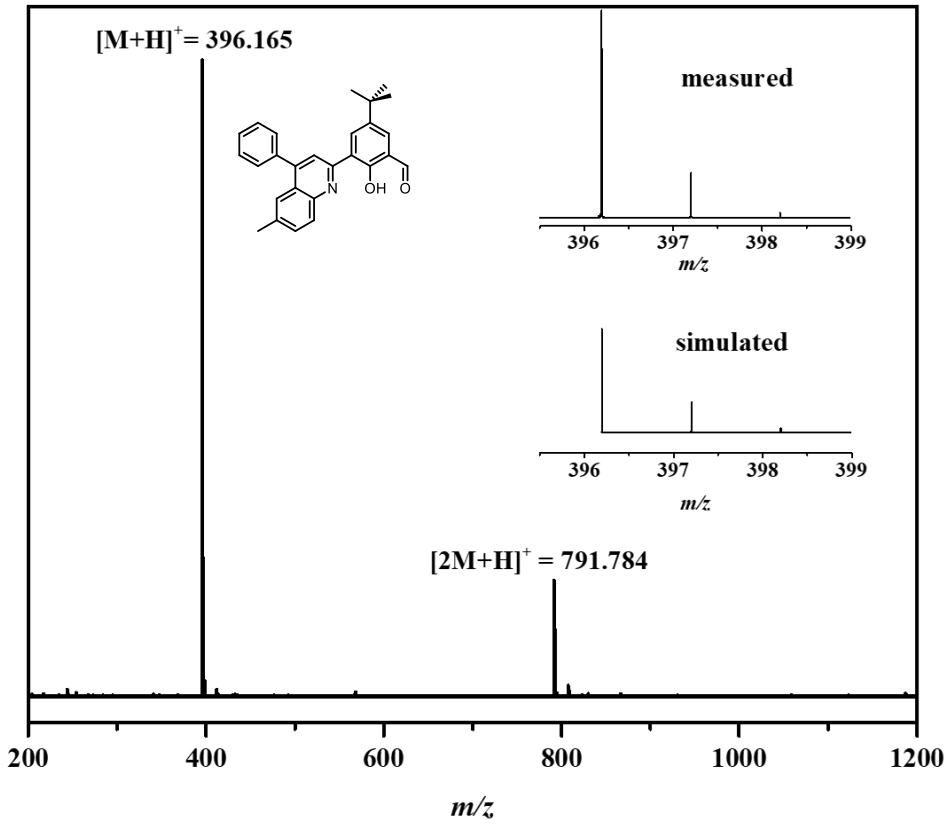

Figure S17. HRMS (DART) of **S2.**

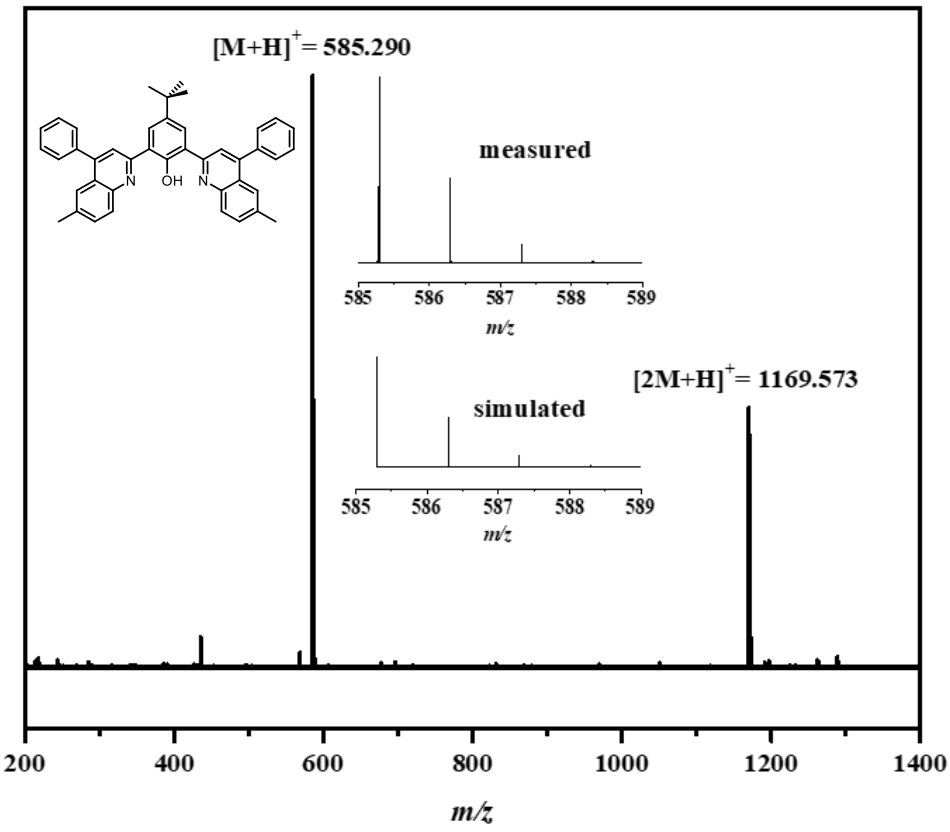

Figure S18. HRMS (ESI) of model compound **3**.

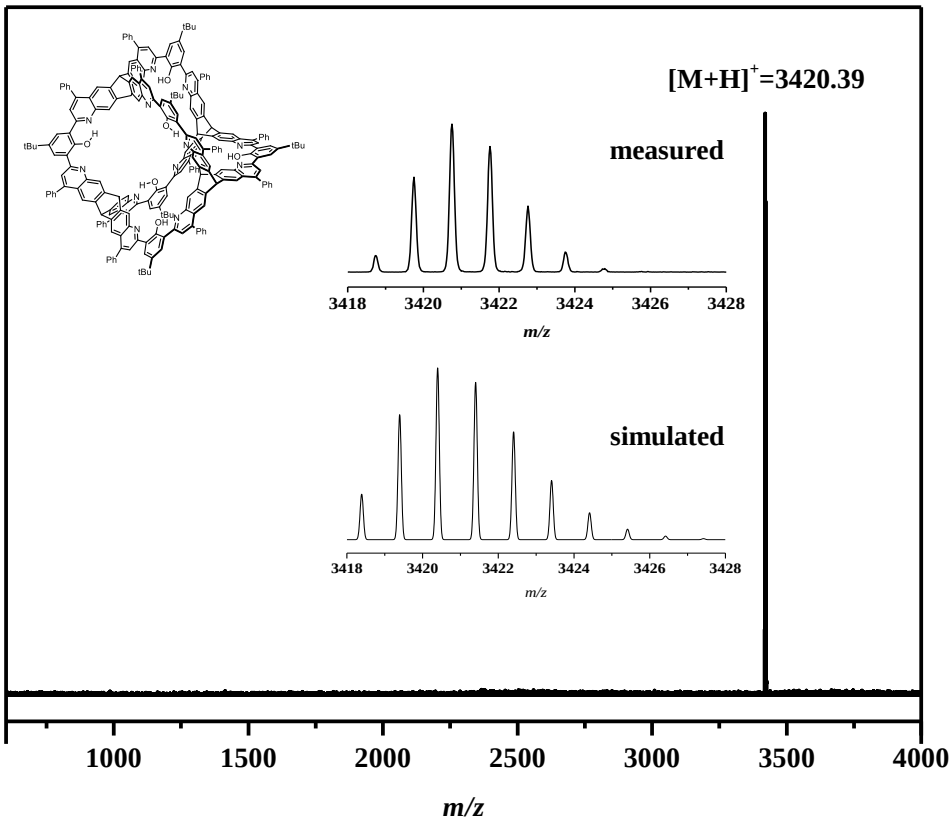

Figure S19. MALDI-TOF MS (DCBT) of cage compound **2**.

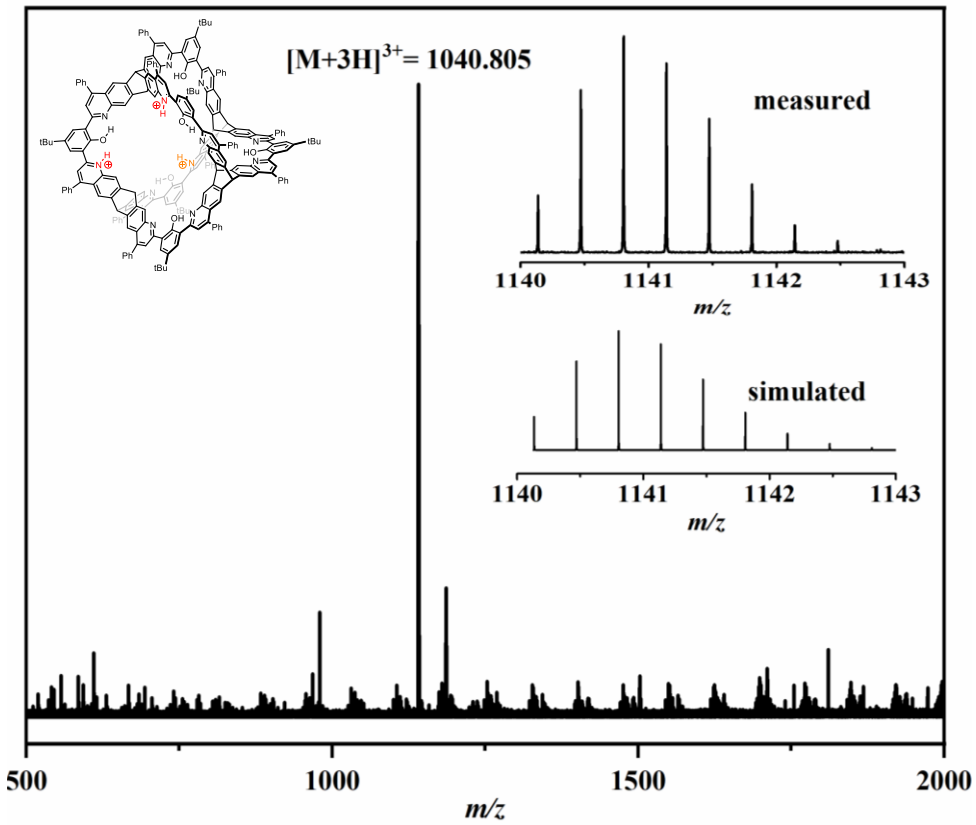

Figure S20. HRMS (ESI) of protonated cage compound **2**. Sample of the cage was dissolved in DCM with an excess of TFA (1.0 10^5 eq.)

3.4 IR Spectra

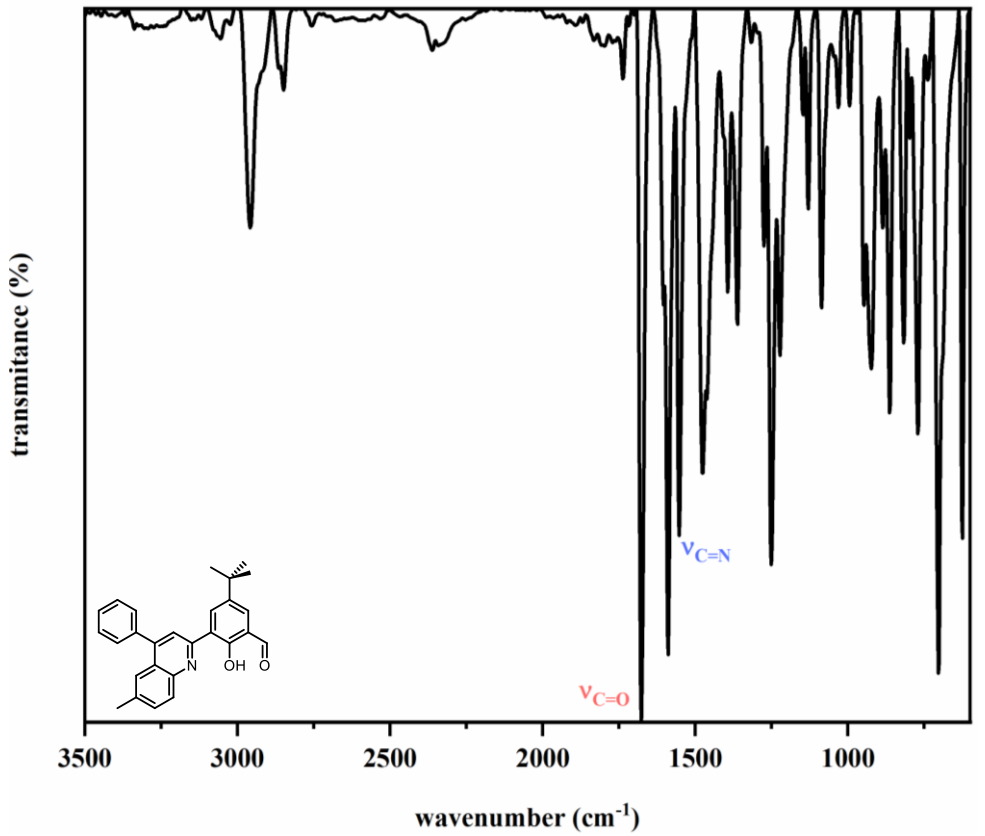

Figure S21. IR (ATR) spectrum of compound **S2**.

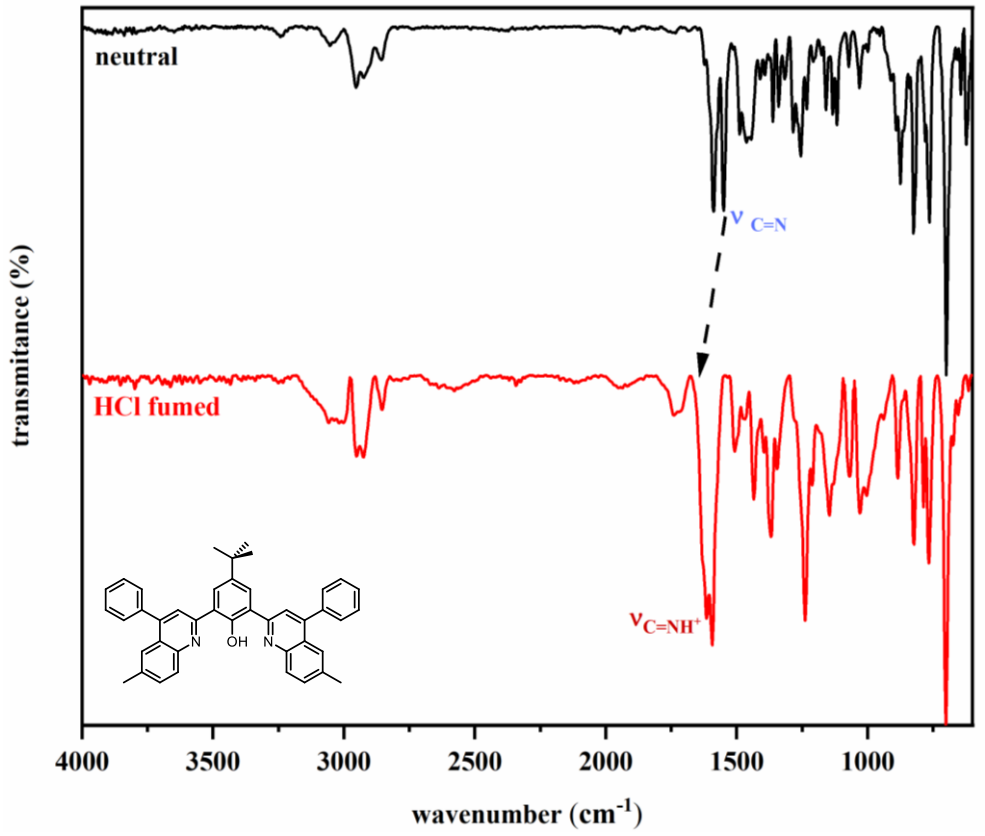

Figure S22. IR (ATR) spectrum of the model compound **3** as synthesized (black) and HCl fumed (red).

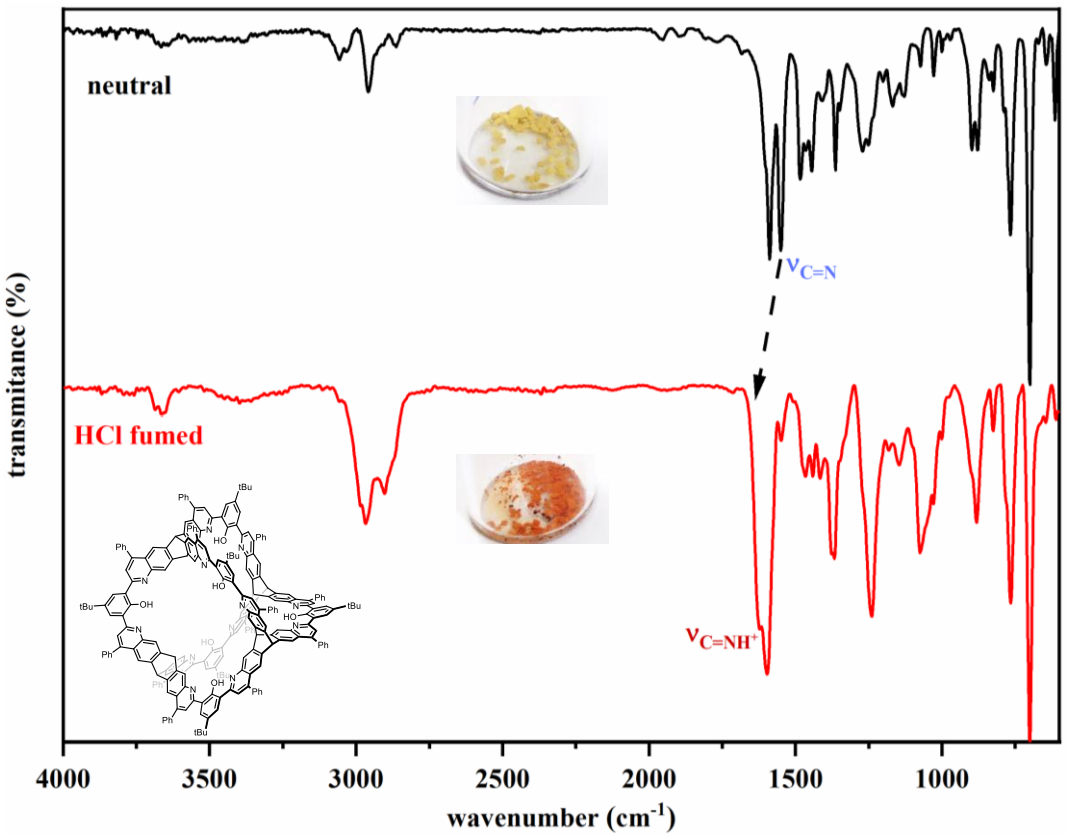

Figure S23. IR (ATR) spectrum of cage compound **2** as synthesized (black) and HCl fumed (red).

3.5 Thermogravimetric Analysis (TGA)

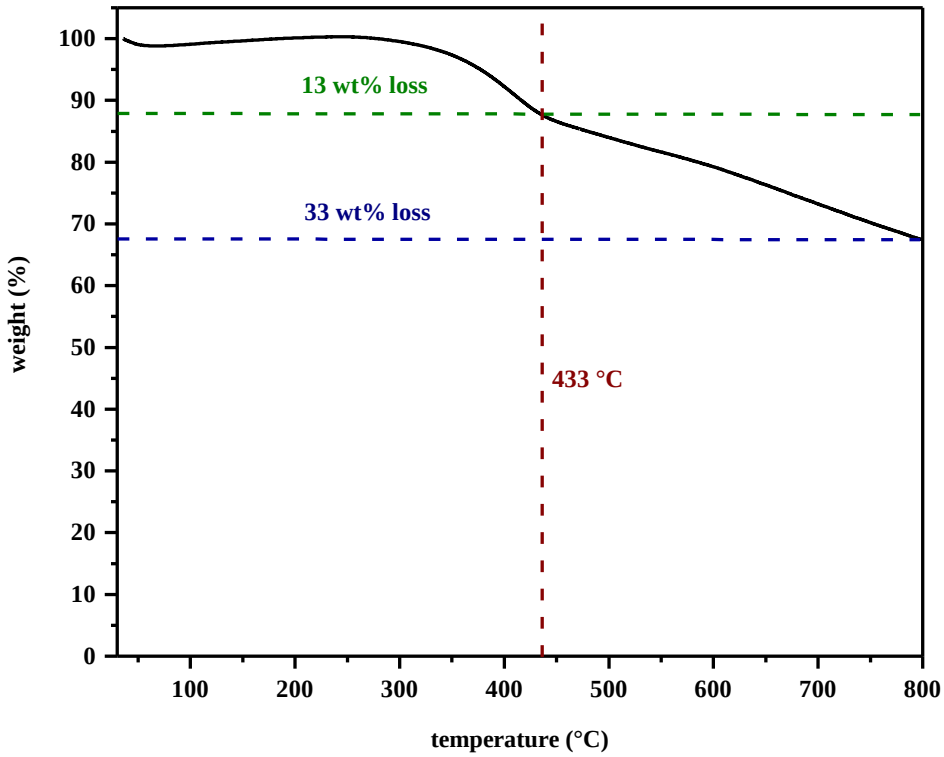

Figure S24. Thermogravimetric analysis of cage compound **2** (N_2, heating rate: 10 °C/min).

4. Crystal Structure Analysis

Crystals suitable for X-ray diffraction were obtained by slow cooling of a solution of **3** in DMSO.

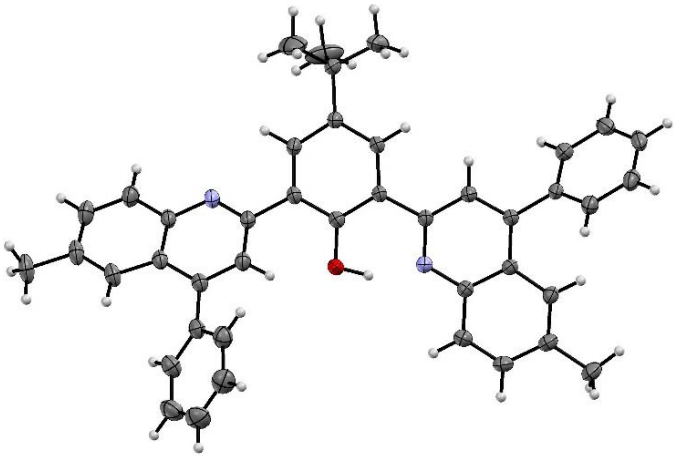

Figure S25. the crystal structure of model compound (**3**) shown with thermal ellipsoids at 50% probability. White : hydrogen, grey: carbon, red: oxygen, blue : nitrogen.

CCDC	2002766
Empirical formula	$C_{42}H_{36}N_2O$
Formula weight	584.73
Temperature	200(2) K
Wavelength	0.71073 Å
Crystal system	monoclinic
Space group	$P2_1/n$
Z	4
Unit cell dimensions	a = 16.0311(16) Å α = 90 deg. b = 12.3469(12) Å β = 106.8879(16) deg. c = 16.6684(16) Å γ = 90 deg.
Volume	3157.0(5) $Å^3$
Density (calculated)	1.23 g/cm^3
Absorption coefficient	0.07 mm^{-1}
Crystal shape	brick
Crystal size	0.189 x 0.167 x 0.102 mm^3
Crystal colour	orange
Theta range for data collection	1.6 to 30.6 deg.
Reflections collected	43038
Independent reflections	9683 (R(int) = 0.0588)
Observed reflections	5934 ($I > 2\sigma(I)$)
Absorption correction	Semi-empirical from equivalents
Max. and min. transmission	0.96 and 0.88
Refinement method	Full-matrix least-squares on F^2
Data/restraints/parameters	9683 / 0 / 415
Goodness-of-fit on F^2	1.04
Final R indices ($I>2\sigma(I)$)	R1 = 0.058, wR2 = 0.134
Largest diff. peak and hole	0.35 and -0.32 $eÅ^{-3}$

Crystals suitable for X-ray diffraction were obtained by diffusion of ammoniac EtOAc mixture into a solution of cage compound **2** in DCM at room temperature

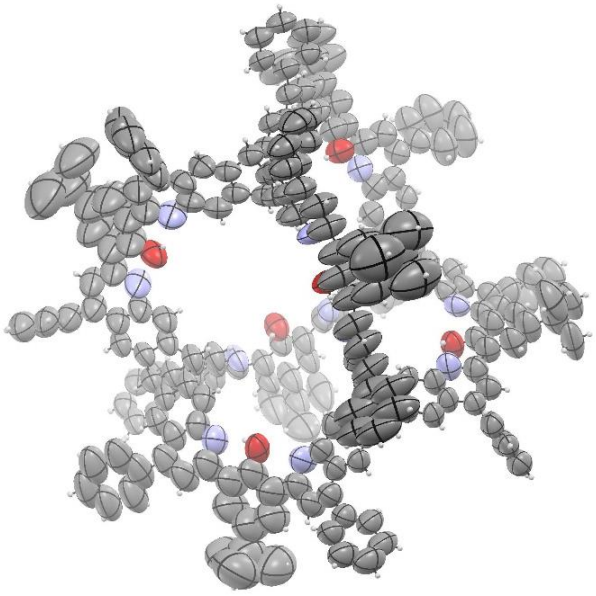

Figure S26. Crystal structure of cage compound (**2**) shown with thermal ellipsoids at 50% probability. White : hydrogen, grey: carbon, red: oxygen, blue: nitrogen.

CCDC	2002767	
Empirical formula	$C_{248}H_{176}N_{12}O_6$	
Formula weight	3420.00	
Temperature	200(2) K	
Wavelength	1.54178 Å	
Crystal system	cubic	
Space group	$P\bar{4}3n$	
Z	8	
Unit cell dimensions	a = 42.8035(5) Å	α = 90 deg.
	b = 42.8035(5) Å	β = 90 deg.
	c = 42.8035(5) Å	γ = 90 deg.
Volume	78422(3) $Å^3$	
Density (calculated)	0.58 g/cm^3	
Absorption coefficient	0.27 mm^{-1}	
Crystal shape	cubic	
Crystal size	0.250 x 0.185 x 0.127 mm^3	
Crystal colour	orange	
Theta range for data collection	2.1 to 40.0 deg.	
Reflections collected	80666	
Independent reflections	7936 (R(int) = 0.0463)	
Observed reflections	5035 ($I > 2\sigma(I)$)	
Absorption correction	Semi-empirical from equivalents	
Max. and min. transmission	1.31 and 0.63	
Refinement method	Full-matrix least-squares on F^2	
Data/restraints/parameters	7936 / 2198 / 681	
Goodness-of-fit on F^2	1.00	
Final R indices ($I>2\sigma(I)$)	R1 = 0.051, wR2 = 0.146	
Absolute structure parameter	0.50(6)	
Largest diff. peak and hole	0.08 and -0.09 $eÅ^{-3}$	

4.1 Powder X-ray Diffraction (PXRD)

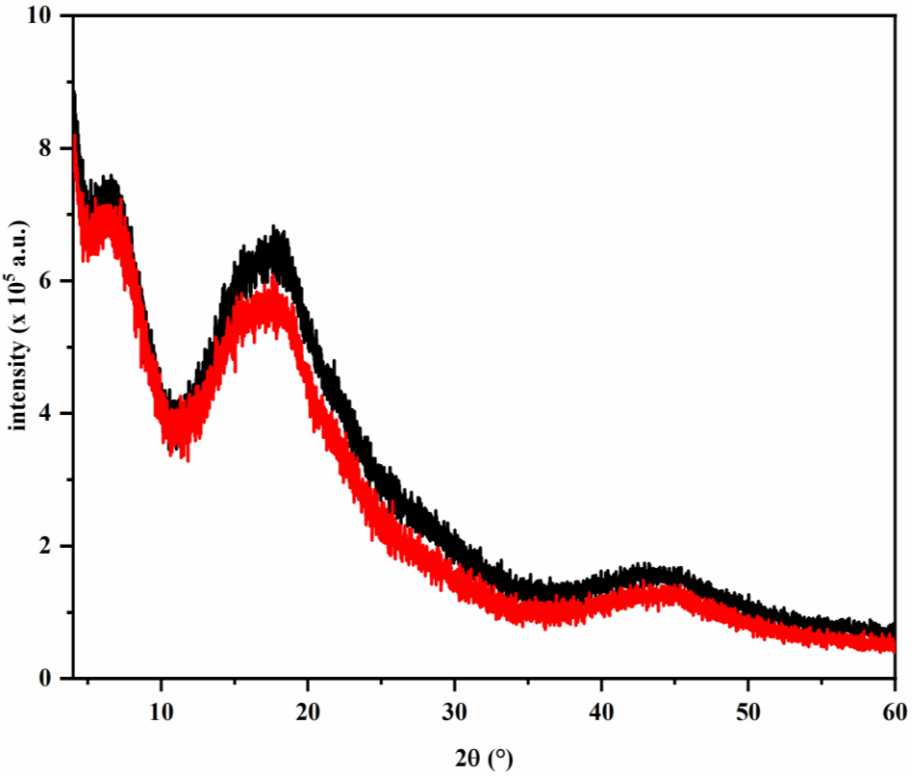

Figure S27. Powder X-ray diffractogram of the cage compound **2** before gas sorption measurements (black) and after the measurements (red).

5. Scanning Electron Microscopy (SEM)

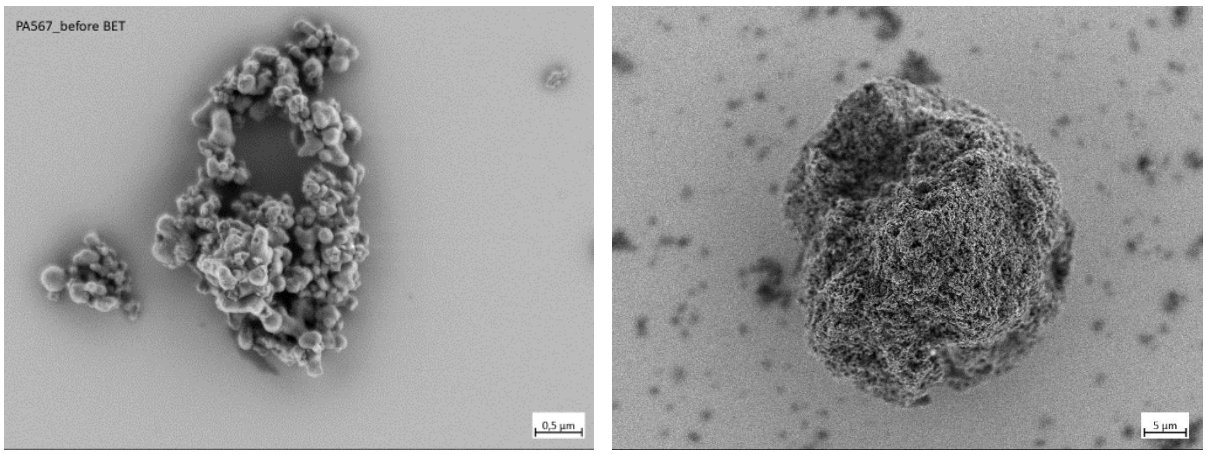

Figure S28.SEM micrograph of batch 1 of the cage compound **2** before BET measurements

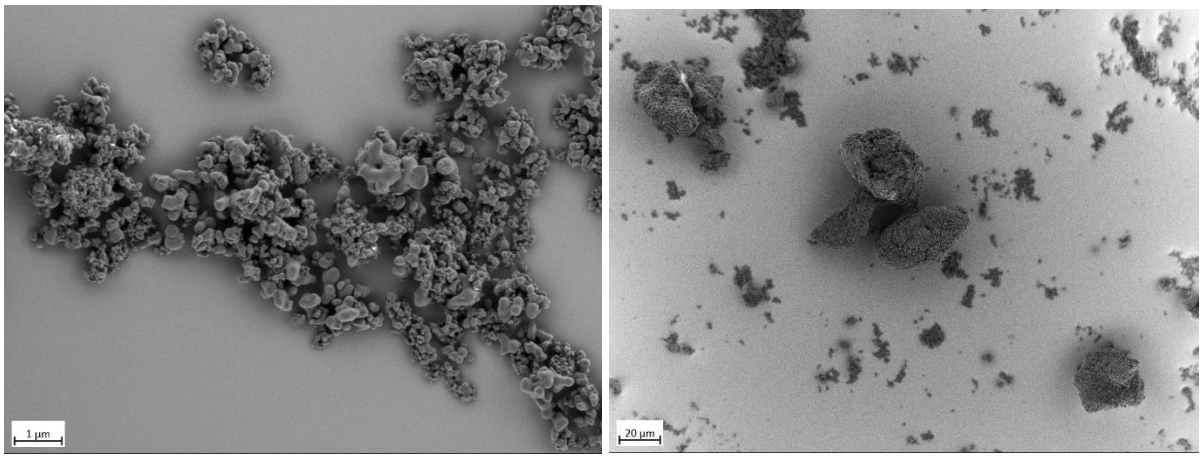

Figure S29. SEM micrograph of batch 2 of the cage compound **2** after BET measurements

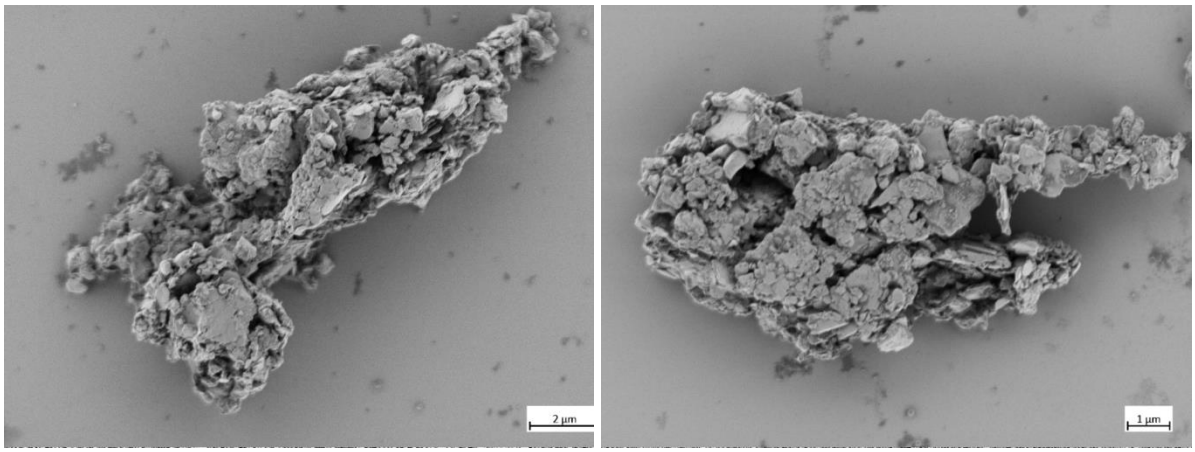

Figure S30. SEM micrograph of the cage compound **2** obtained from recrystallization in chloroform

6. Gas Sorption Data (BET)

Activation of the cage compound **2** for gas sorption: 40 to 100 mg of the cage compound was immersed in Et_2O (2 x 5 mL) and in n-pentane (5 x 5 mL). The solid was dried overnight under high vacuum ($1.0 \cdot 10^{-3}$ mbar) at 250 °C before transferring to the gas sorption analyzer.

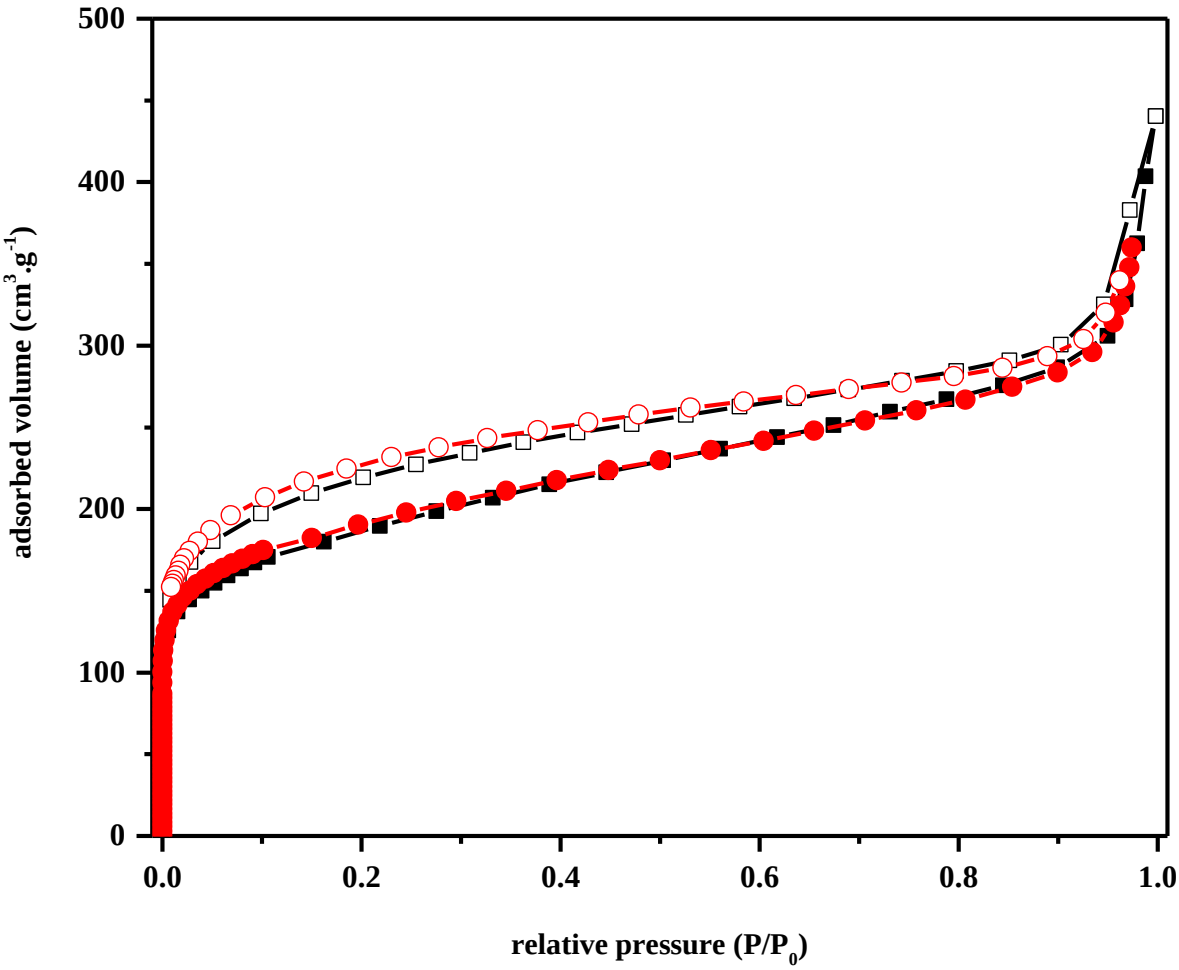

Figure S31. Nitrogen adsorption (batch 1: black filled squares, batch 2: red filled circles) and desorption (batch 1: black hollow squares, batch 2: red hollow circles) isotherms of cage compound **2** measured at 77 K.

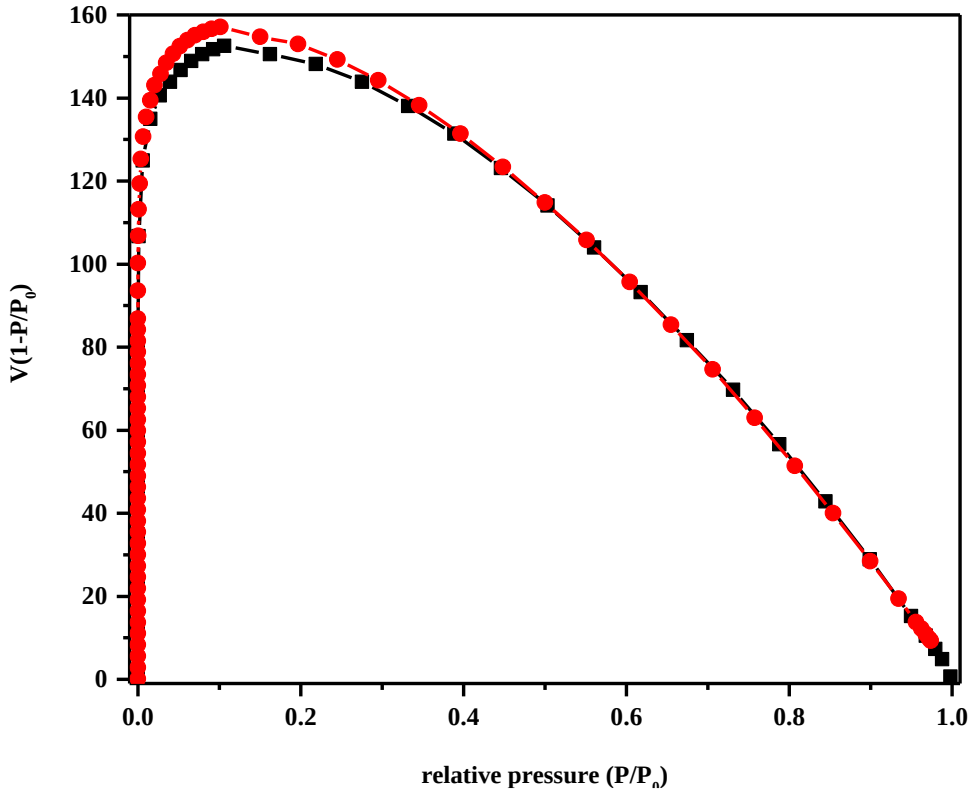

Figure S32. Rouquerol-plots (batch 1: black squares, batch 2: red circles) of cage compound **2**.

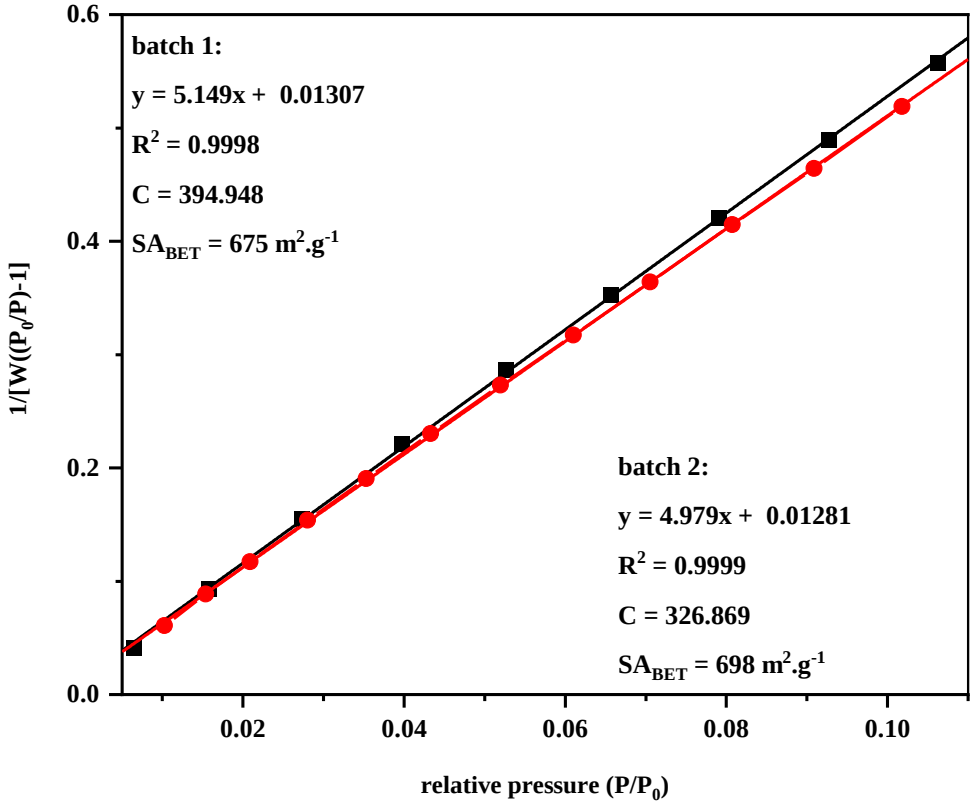

Figure S33. BET-plots (batch 1: black squares, batch 2: red circles) of the cage compound **2**. The calculated surface area is 675 $m^2 \cdot g^{-1}$ for batch 1 and 698 $m^2 \cdot g^{-1}$ for batch 2.

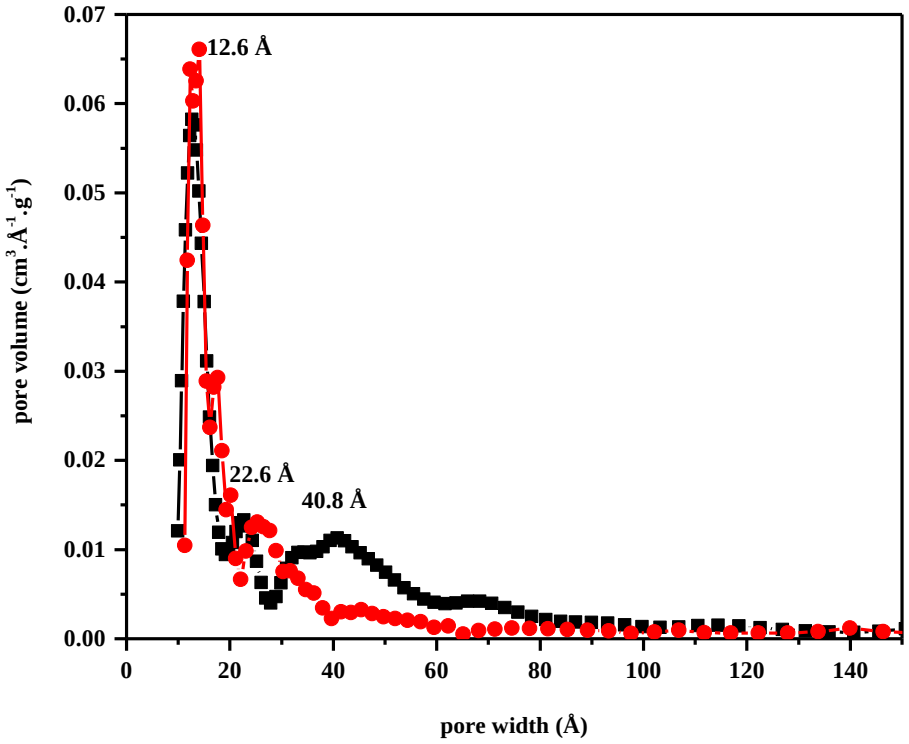

Figure S34. QS-DFT (spherical/cylindrical pores, N_2 at 77 K on carbon) pore size distribution plots (batch 1: black squares, batch 2: red circles) of cage compound **2**.

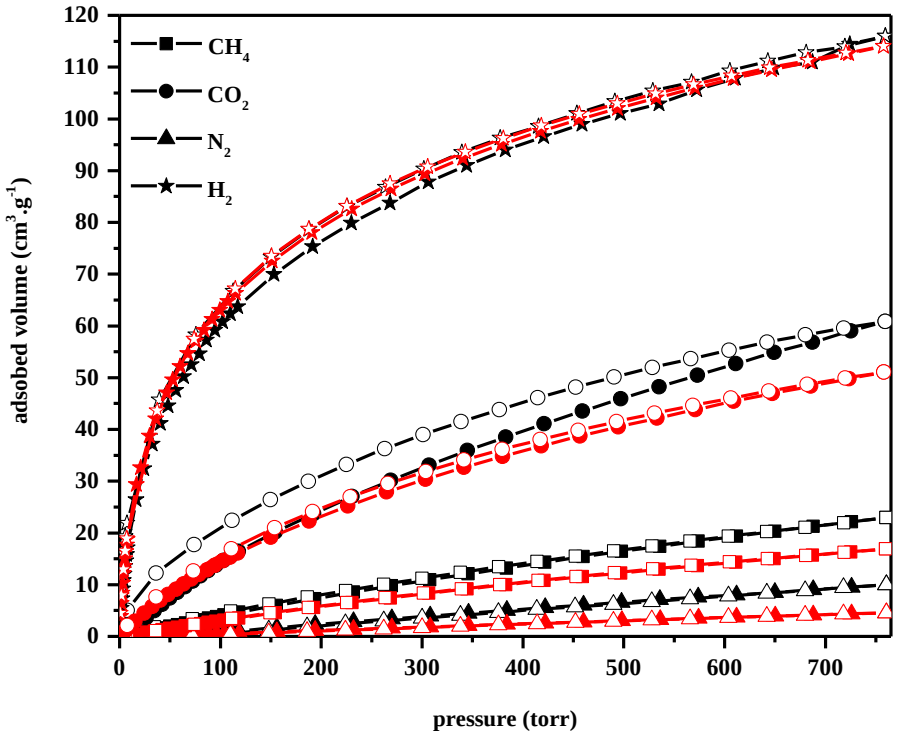

Figure S35. Gas sorption isotherms of cage compound **2** (batch 1: black, batch 2: red) measured at 273 K for methane (squares), carbon dioxide (cycles), nitrogen (triangles) and at 77K for hydrogen (asterisks). The adsorption is represented as filled symbols and desorption as hollow symbols. The uptake of carbon dioxide is 12 wt%, of methane 1.85 wt%, of hydrogen 1.0 wt% for batch 1. The uptake of carbon dioxide is 10 wt%, of methane 1.20 wt%, of hydrogen 1.0 wt% for batch 2.

7. Calculation of Isosteric Heat of Adsorption

A virial-type expression comprising the temperature-independent parameters a_i and b_i was used to calculate the enthalpies of adsorption for CO_2 and CH_4 on the cage compound **2** (at 263 K and 273 K). In each case, the data were fitted using the following equation:

Equation S2: $$\ln(p) = \ln(q) + \frac{1}{T}\sum_{i=0}^{m}(a_i * q^i)\sum_{i=0}^{m}(b_i * q^i)$$

where: - p is the pressure (torr)

- q is the amount of gas adsorbed (mol.kg^{-1})

- T is the temperature (K)

- a_i and b_i are virial coefficients

- n and m the number of coefficients required to adequately describe the isotherms.

The number of coefficients (n and m) were gradually increased until the contribution of extra added a and b coefficients was deemed to be statistically insignificant towards the overall fit, and the average value of the squared deviations from the experimental values was minimized ($m \leq 6$, $n \leq 3$). The values of the virial coefficients a_0 through a_m were then used to calculate the isosteric heat of adsorption using the following expression.

Equation S3: $$Q_{st} = -R\sum_{i=0}^{m}(a_i * q^i)$$

where: - Q_{st} is the coverage-dependent isosteric enthalpy of adsorption (J.mol^{-1})

- R is the universal gas constant (J.K^{-1}.mol^{-1})

- q is the amount of gas adsorbed (mol.kg^{-1})

- a_i is a virial coefficient

- m is the number of coefficients required to adequately describe the isotherms.

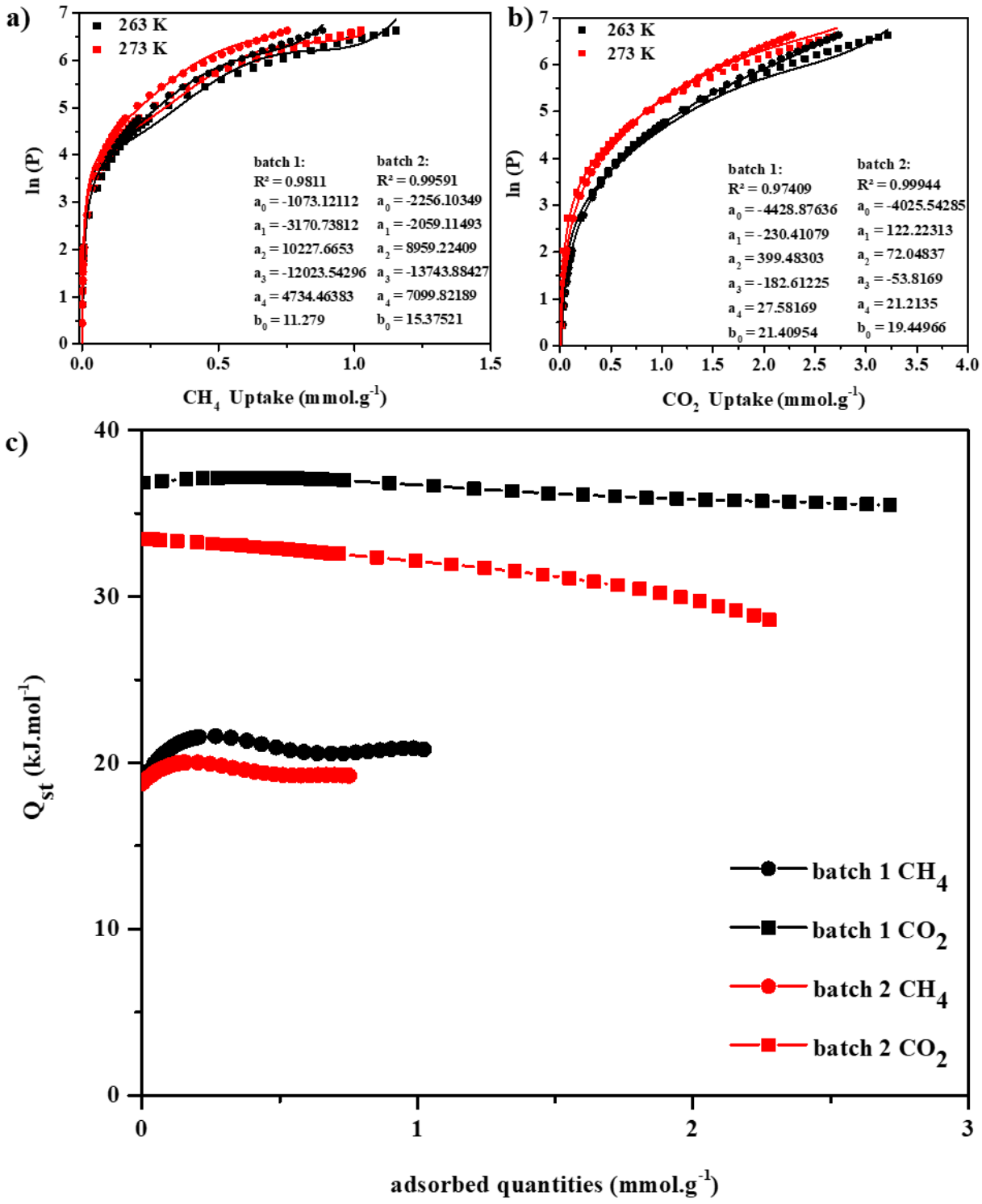

Figure S36. a) CO2 isotherms and virial fitting curves for the cage compound **2**. Red: 273K. Black: 263K.b) CH_4 isotherms and virial fitting curves for cage compound **2**. Red: 273K. Black: 263K. c) calculated heat of adsorption curve of the cage compound 2 for carbon dioxide (black) and methane (red).

8. Calculation of Selectivity by Henry's Law

The non-linear Tóth equation was fit to the measured isotherms of CO_2 and CH_4 adsorptions at 263 K and 273 K:

Equation S4: $$n = n_s \frac{b^{1/t} * p}{(1 + b * p^t)^{1/t}}$$

Where: - n is the amount of gas adsorbed ($mol \cdot kg^{-1}$)

- n_s is the saturation uptake ($mol \cdot kg^{-1}$)

- p is the pressure (torr)

- t and b are parameters which are specific for adsorbate-adsorbent pairs

With the obtained parameters, the Henry's law constant K_H was calculated. K_H quantifies the extent of adsorption of an adsorbing gas by a solid material. Henry's law constant is defined by the following equation:

Equation S5: $$K_H = \lim_{p \to 0} \frac{dn}{dp} = b^{1/t} * n_s$$ for a Tóth isotherm.

By using the parameters derived from fitting equation S4 to the isotherms in equation S5. The Henry's law constant was calculated for methane and carbon dioxide at 273 K.

Table S1: parameters of the adjustments of non-linear Tóth isotherms to the experimental data of gas sorption measurements and Henry´s law constants of the cage compound **2** for batch 1 and 2.

Cage 2	***T* [K]**	**Gas**	**Affinity constant [bar^{-1}]**	**Maximal loading [$mmol.g^{-1}$]**	**Tóth-exponent**	**R^2**	**K_H [$mmol.g^{-1}.bar^{-1}$]**
Batch 1	273	N_2	7.03561	3.62568	5.59359	0.99072	5.13885
Batch 2	273	N_2	8.16605	2.16396	3.96892	0.99804	3.67314
Batch 1	273	CO_2	0.68965	10.73506	0.64369	0.99879	6.02708
Batch 2	273	CO_2	0.97369	8.96965	0.51237	0.99998	8.51483
Batch 1	273	CH_4	0.32496	4.97745	0.8821	0.9999	1.3918
Batch 2	273	CH_4	0.41295	2.8211	0.92354	0.99994	1.08271

9. Evaluation of the screening experiments on cage 2

All screening reactions were performed with 10 mg cage **2** (5 μmol), 7.9 mg $Sc(OTf)_3$ (0.02 mmol, 3.6 eq.) and 13.3 mg chloranil (0.05 mmol, 12 eq.) in screw-cap vials (1 mL) at 100 °C with phenylacetylene (0.5 mL). MALDI-TOF measurements were performed by removing a few drops of the reaction mixture directly from the reaction vessel and measured per MALDI-TOF immediately without further treatment.

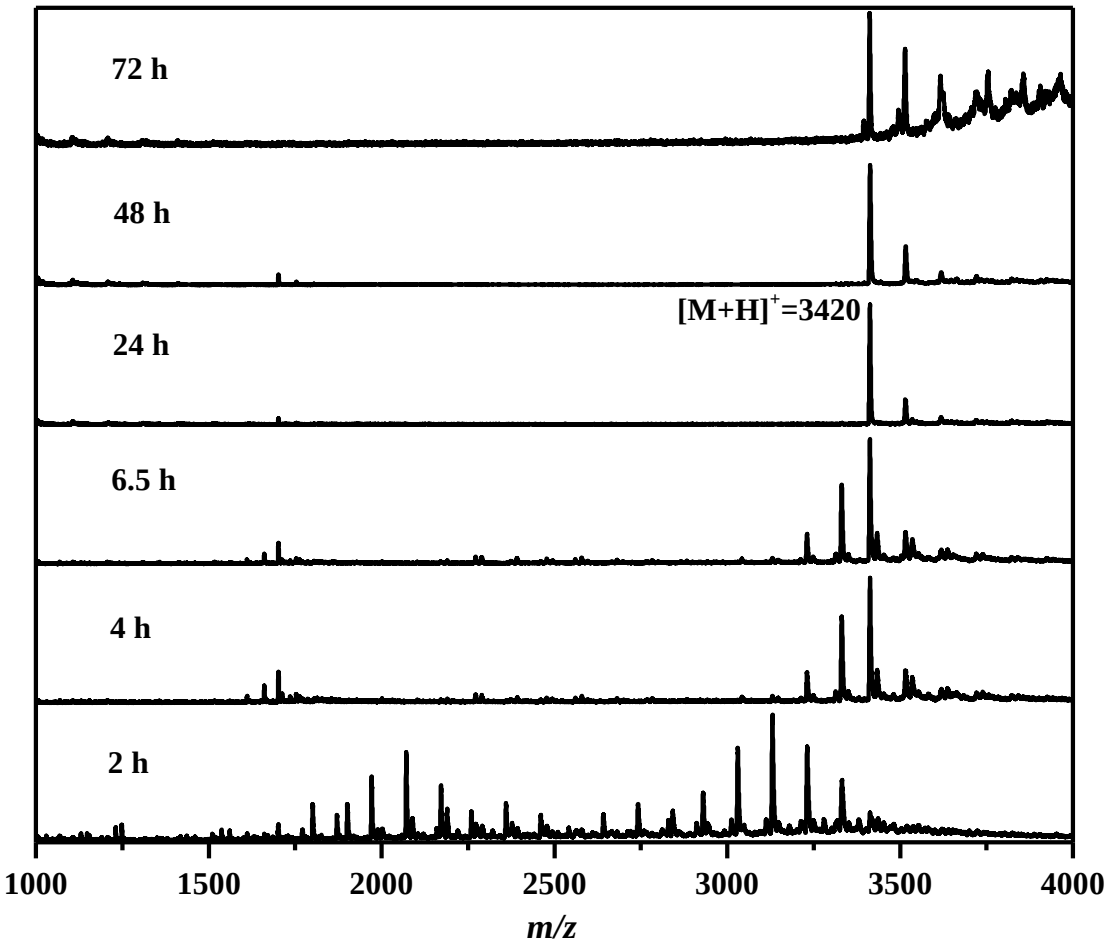

Figure S37. Time depended MALDI-TOF MS (DCBT) investigations of the formation of cage compound **2**.

10. Chemical Stability Tests

Imine Cage 1: ~5.0 mg of the imine cage compound **1** was stirred in different aqueous solutions (3 mL) of varying pH. All samples were stirred at r.t (20-25 °C) for 22 hours. The suspensions were diluted with water, filtered, washed with tetrahydrofuran (1 mL), methanol (1 mL) and Et_2O (10 mL) and dried in vacuo before analyzed.

Table S2. Stability test of the cage compound **1** in aqueous solutions of different pH.

Solution	pH	Remarks*	Weight before test	Weight after test
3M H_2SO_4	-0.78	The solid and the solution turned red	5.1 mg	0.8 mg
3M HCl	-0.48	The solid and the solution turned red	5.3 mg	1.2 mg
Water + AcOH (9.8 μL)	3	The solution turned slightly orange	7.8 mg	2.9 mg
water	7	The solution turned slightly orange	4.3 mg	3.5 mg
Water + TEA (0.7 μL)	11	The solution turned slightly orange	7.6 mg	6.2 mg
3M NaOH	14.5	The solution turned slightly orange	5.1 mg	2.2 mg
15M NaOH	15.2	The solution turned slightly orange	4.6 mg	1.8 mg

*All the solids obtained after the filtration were soluble in THF or MeOH while the cage **1** before the treatment is not soluble is those solvents. It is a sign of the decomposition of cage compound **1** under these conditions.

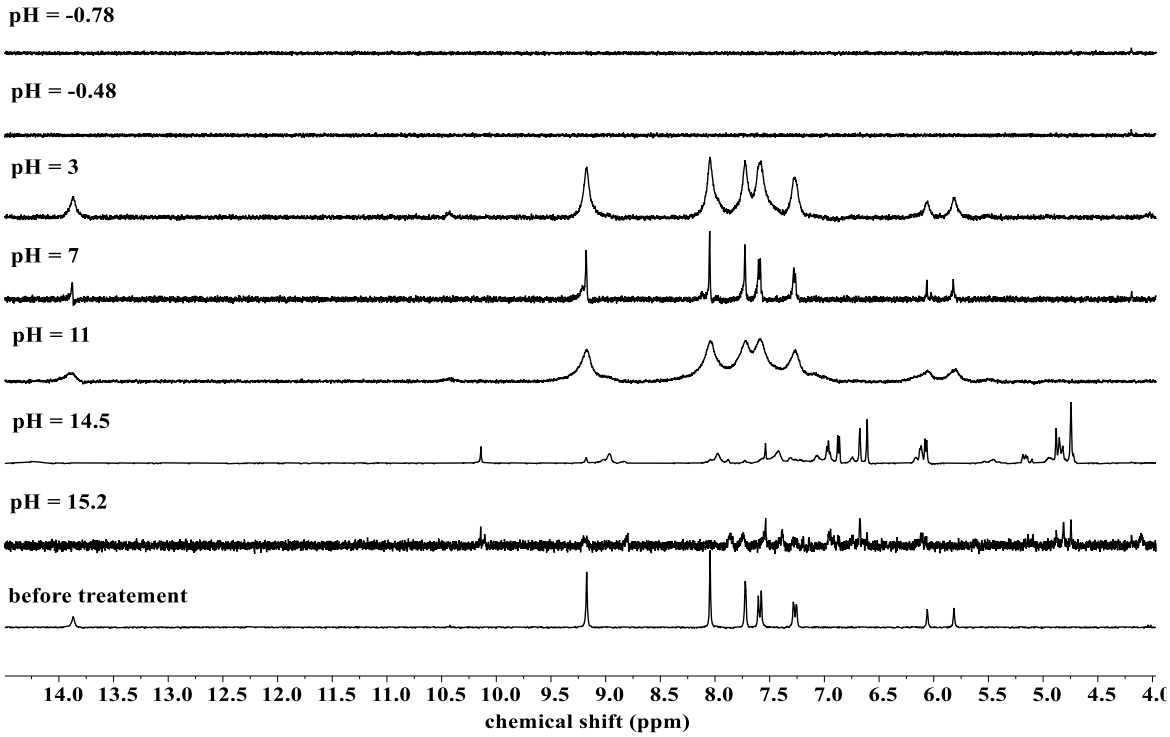

Figure S38. ^{1}H NMR (500 MHz, DMSO-d_6) spectra comparison of the chemical stability test for cage compound **1**. Cage compound is partially stable in a pH-range from 3 to 11.

Quinoline Cage 2: ~5.0 mg of the cage compound **2** was stirred in different aqueous solutions (3 mL) of varying pH. All samples were stirred at r.t (20-25 °C) for 22 hours. The suspensions were diluted with water, collected by filtration, washed with NaOH solution (3 x 8 mL), methanol (3 x 8 mL) and Et_2O (10 mL) and dried in vacuum.

Table S3. Stability test of the cage compound **2** in aqueous solutions of different pH.

Solution	pH	Remarks	Weight before test	Weight after test
36M H_2SO_4	-1.9	Dark brown solution*	5.0 mg	4.5 mg
12M HCl	-1.1	Light brown suspension*	4.8 mg	4.2 mg
15M NaOH	15.2	No change	5.2 mg	6.0 mg

*The solution was poured onto water (20 mL) and a red precipitate was formed.

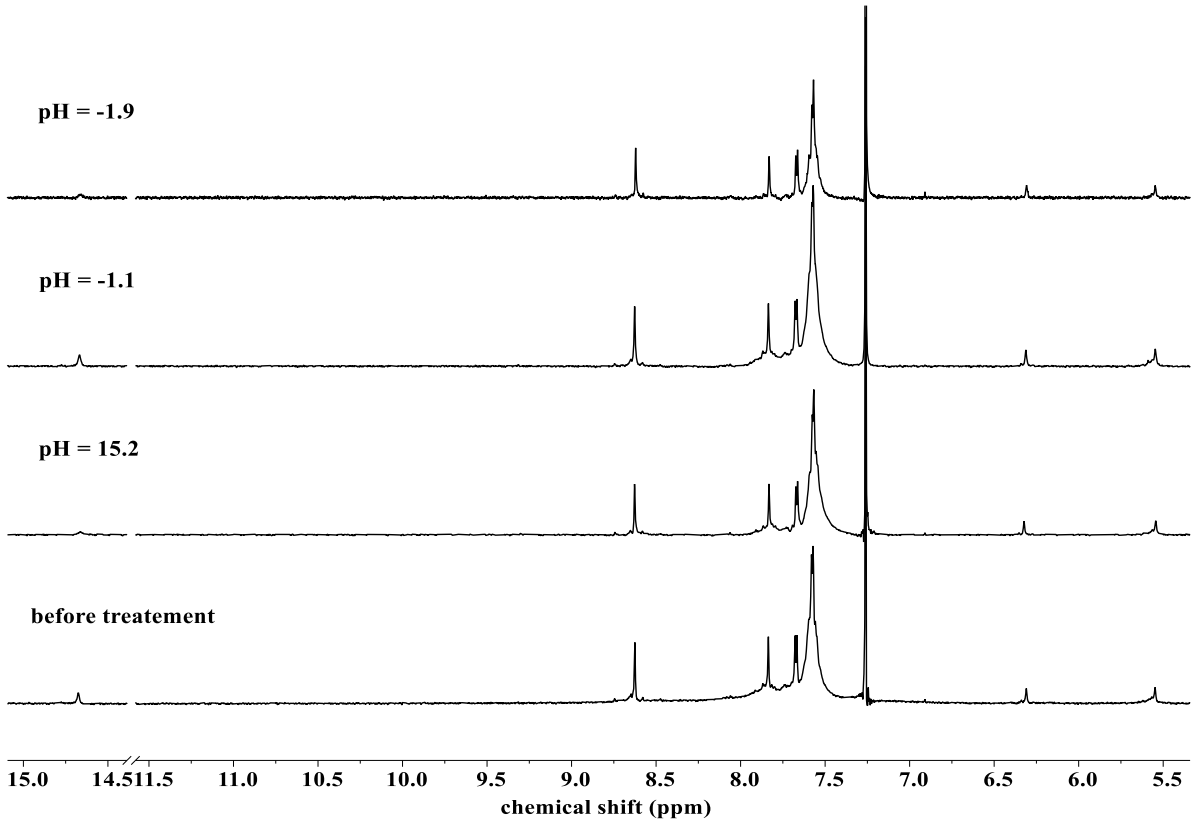

Figure S39. ^1H NMR (300 MHz, $CDCl_3$+0.1 mol% triethyl-d_{15}-amine) spectra comparison of the chemical stability test for cage compound **2**. Cage compound **2** is stable in a broad pH region (pH= -1.9-15.2).

11. Thermal Stability Test

2.5 mg of the cage **2** were placed in a crucible and heated to 350 °C. After cooling to room temperature the solid was dissolved in $CDCl_3$ and ^1H NMR was measured.

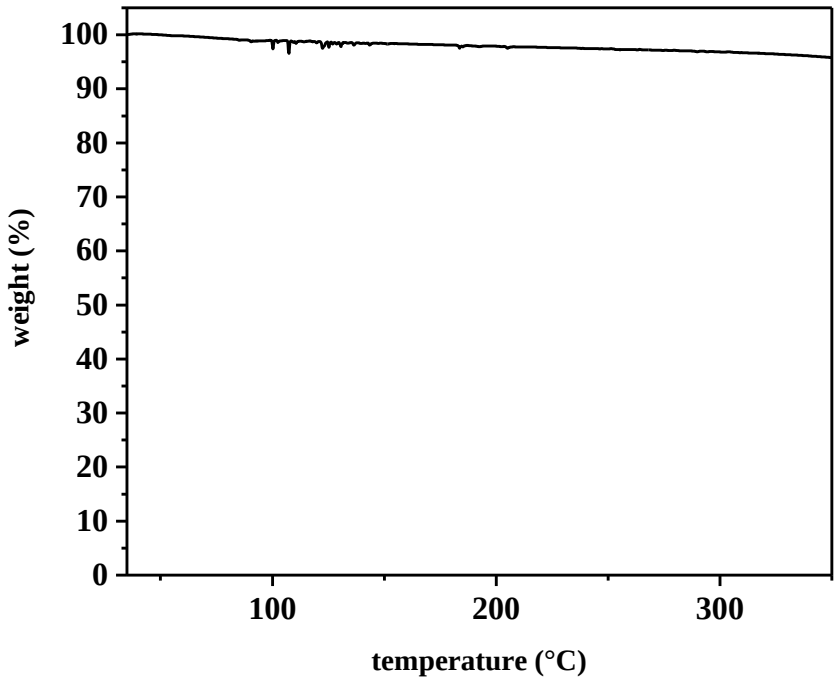

Figure S40. Thermogravimetric analysis of the cage compound **2** (N_2, heating rate: 10 °C/min).

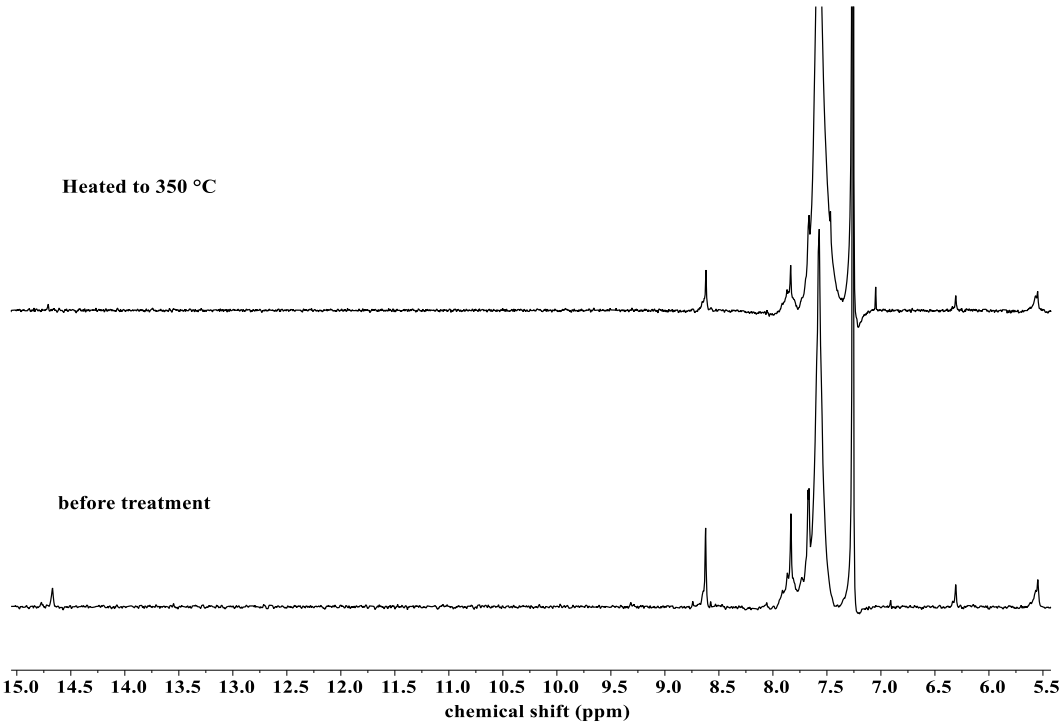

Figure S41. Comparison of ^1H NMR spectra (500 MHz, $CDCl_3$+0.1 mol% triethyl-d_{15}-amine) after the thermal stability test for the cage compound **2**.

12. Absorption and Emission Spectra

12.1 Protonation of the Quinolines – pKb_{DCM}^{TFA} determination

A stock solution (1-4 mg in 20 mL of solvent) of the analyzed compound and stock solutions of acid (acetic acid, trifluoroacetic acid, sulfuric acid, or boron trifluoride etherate) were prepared using the same method. Different aliquots of these stock solutions were mixed in volumetric flasks (10 mL) and filled up to the fill stroke with solvent.

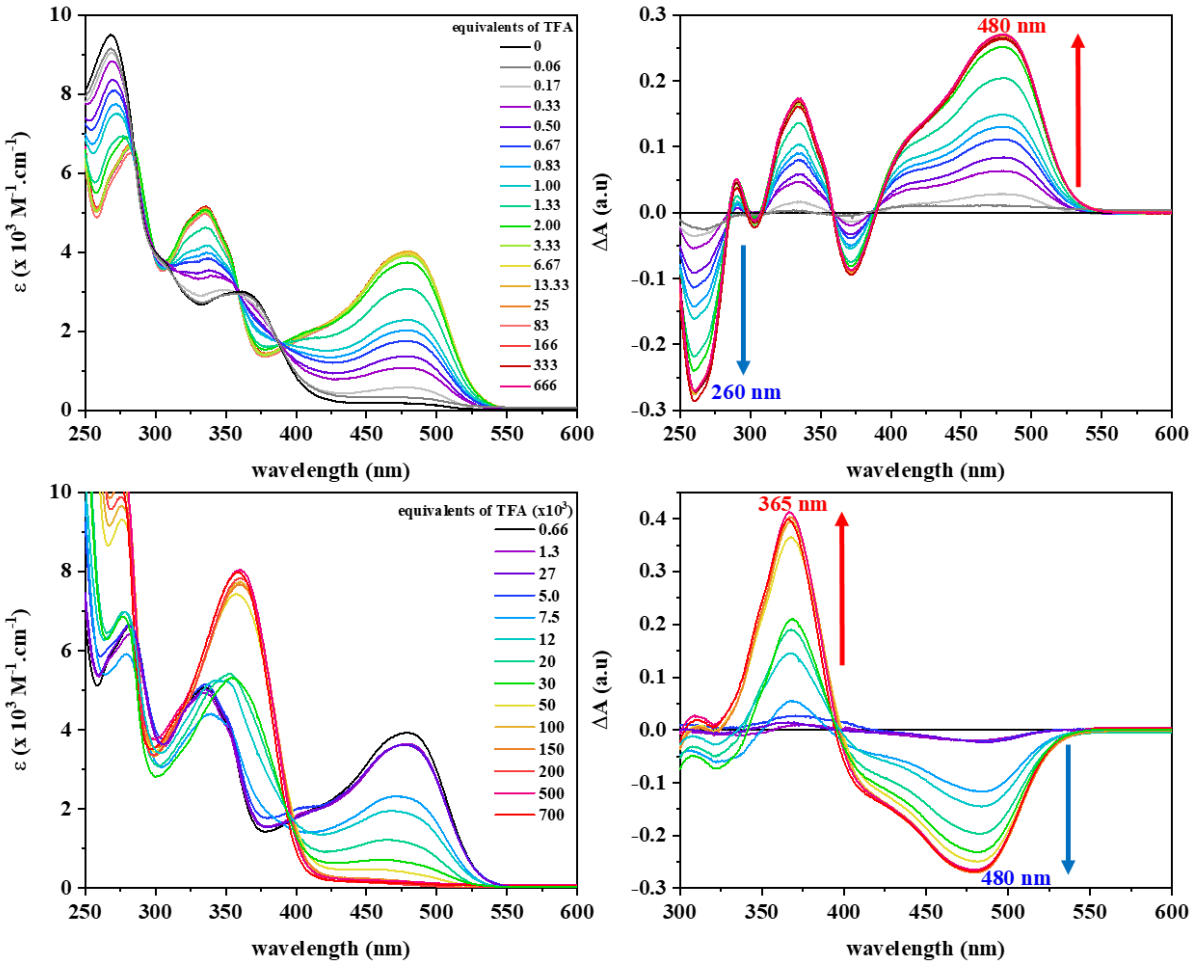

Figure S42. UV/vis titration of model compound **3** with TFA in DCM ($1.48 \cdot 10^{-5}$ mol·L^{-1}). Absorption spectra (left) with different amount of TFA and the corresponding absorption difference spectra (right).

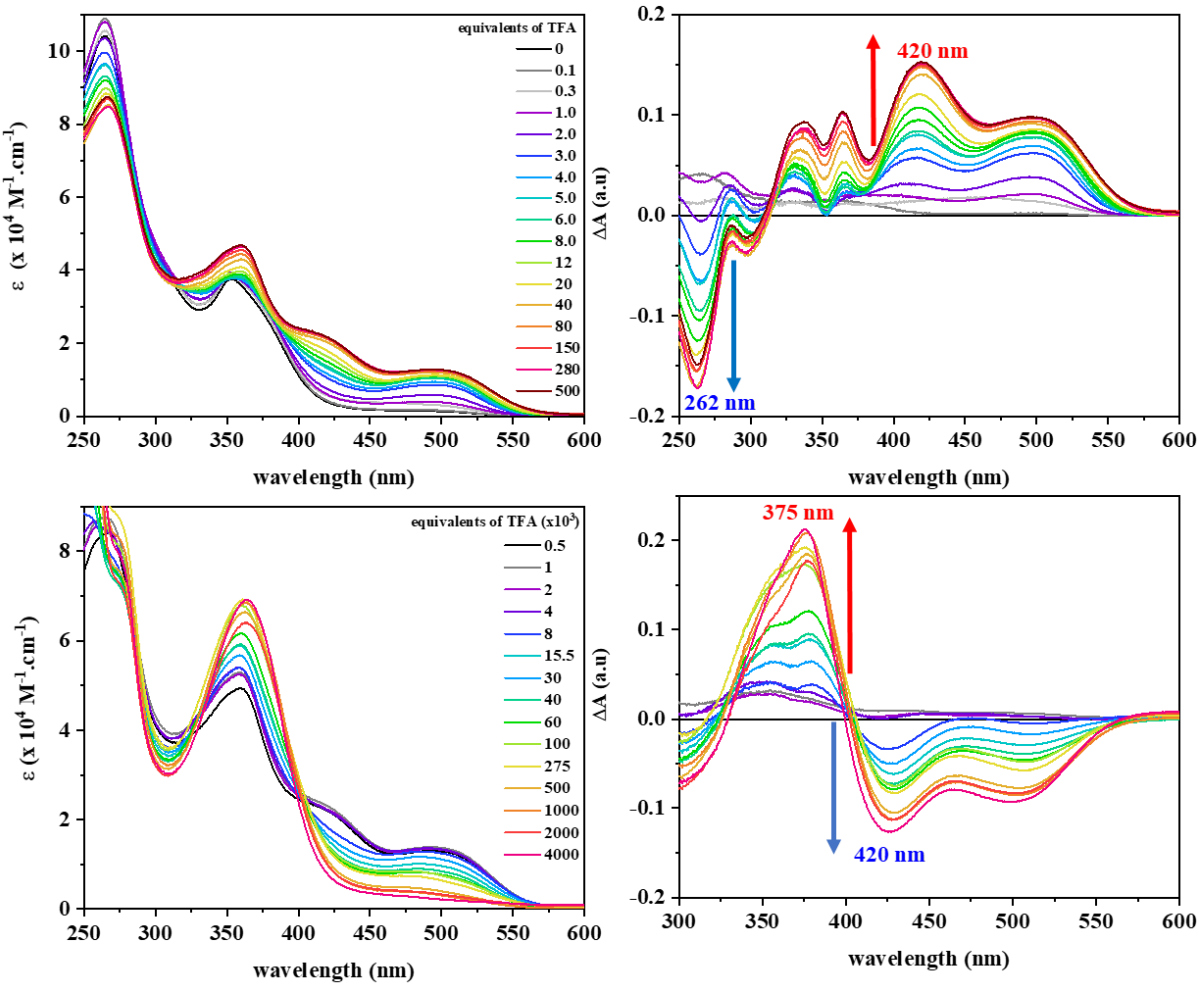

Figure S43. Titration of the cage compound **2** with TFA in DCM ($2.76 \cdot 10^{-6}$ mol·L^{-1}). Absorption spectra (left) with different amount of TFA and the corresponding absorption difference spectra (right).

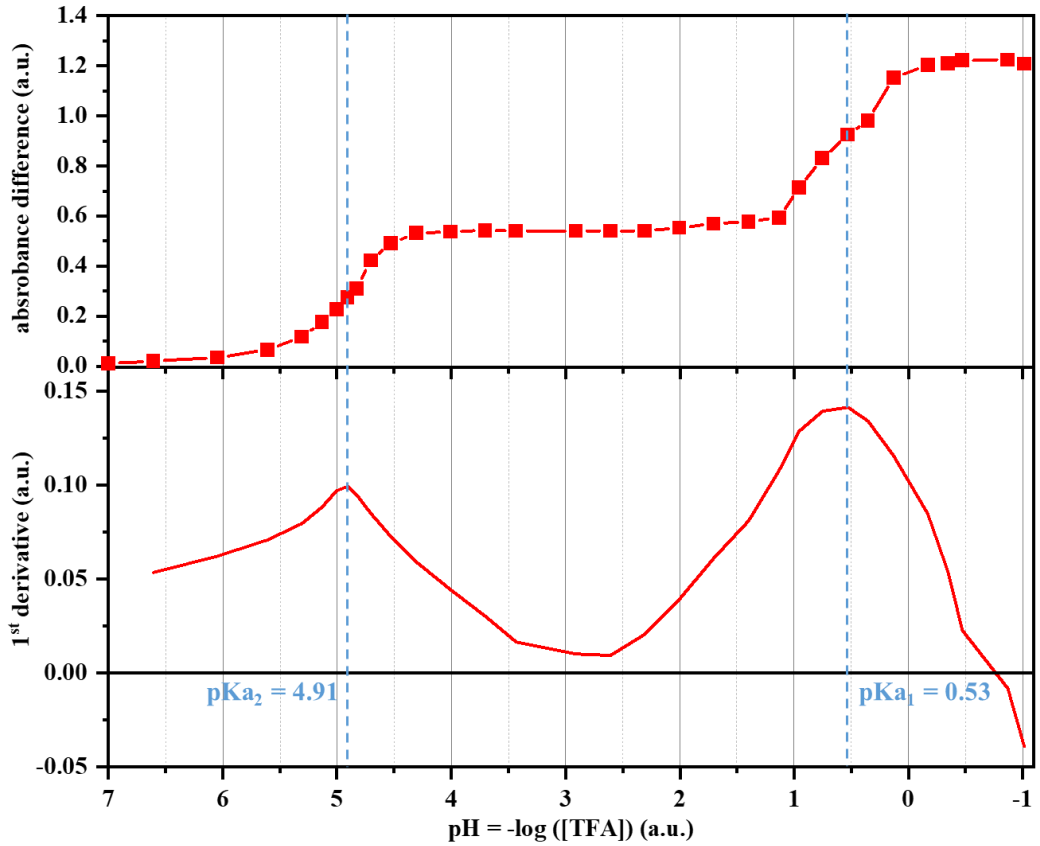

Figure S44. Absorbance difference for the model compound **3** (top) and its first derivative (bottom).

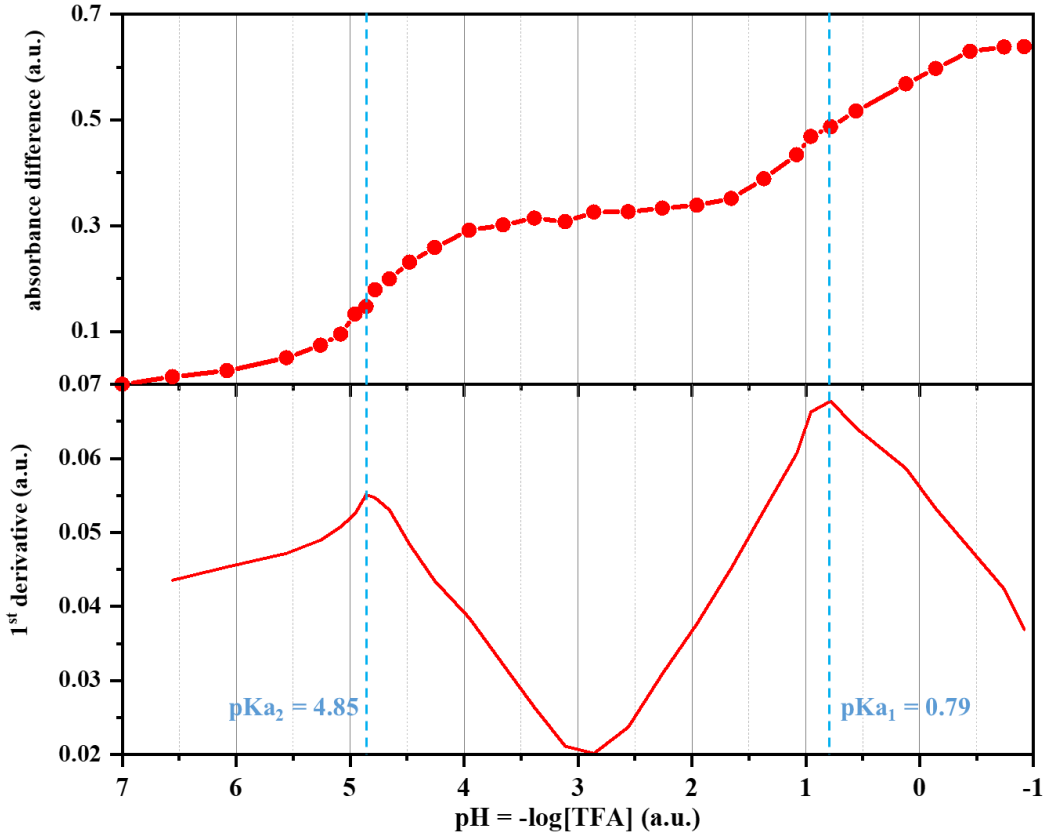

Figure S45. Absorbance difference of the cage compound **2** (top) and its first derivative (bottom).

12.2 Acid-Dependent Protonation in DCM

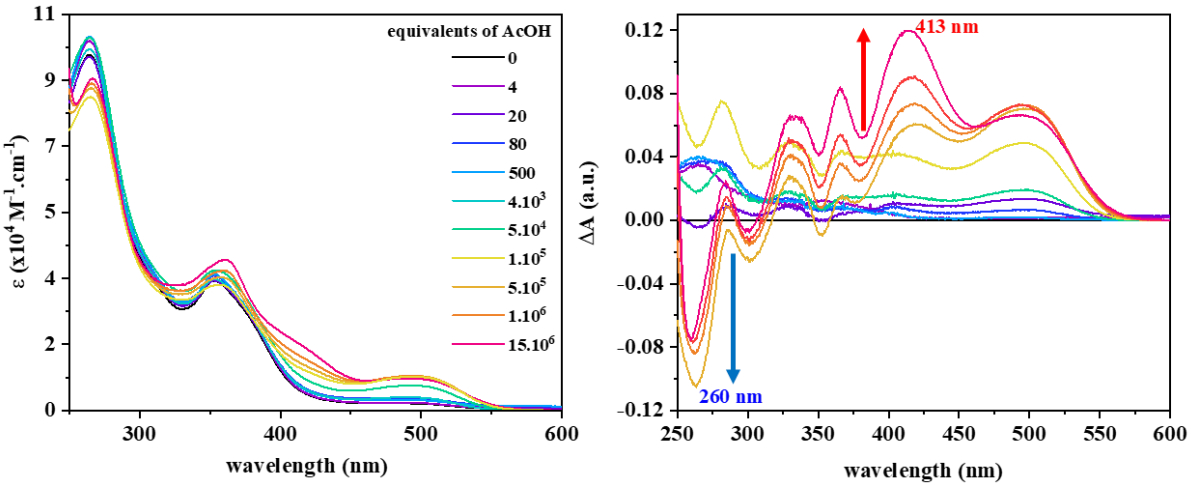

Figure S46. Titration of the cage compound **2** with AcOH in DCM ($2.76 \cdot 10^{-6}$ mol·L^{-1}). Absorption spectra (left) and the corresponding absorption difference spectra (right).

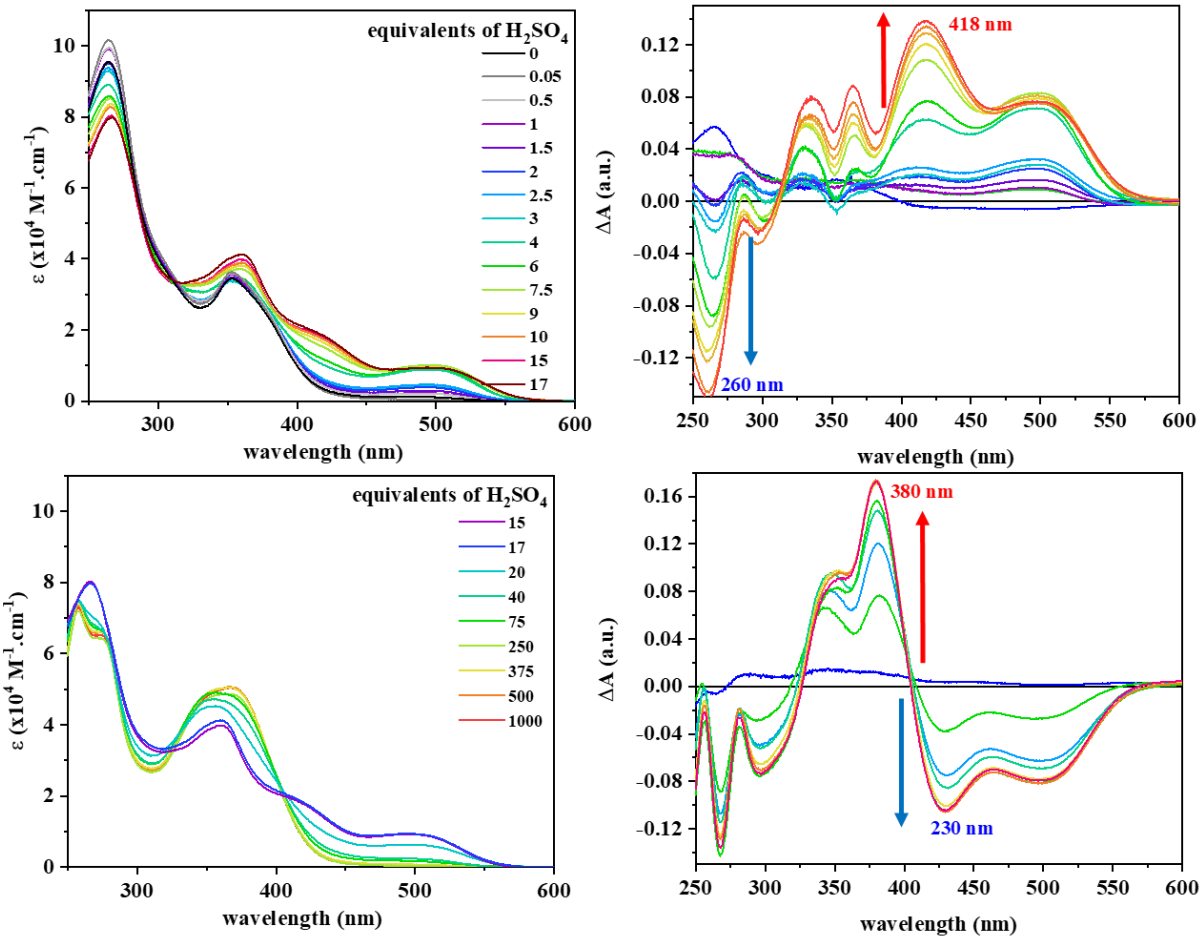

Figure S47. Titration of the cage compound **2** with H_2SO_4 in DCM ($2.76 \cdot 10^{-6}$ mol·L^{-1}). Absorption spectra (left) the corresponding absorption difference spectra (right).

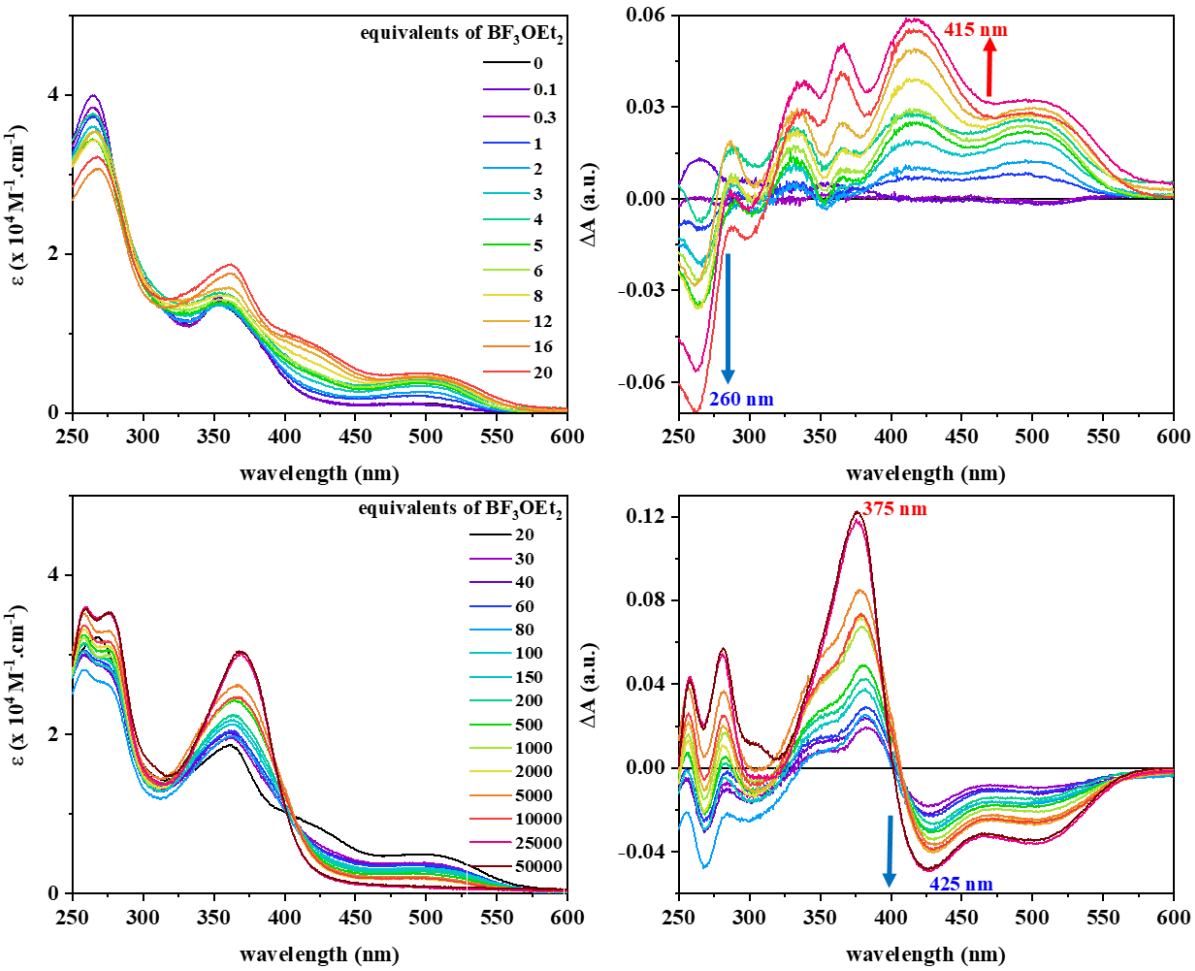

Figure S48. Titration of the cage compound **2** with BF_3OEt_2 in DCM ($1.0 \cdot 10^{-6}$ mol·L^{-1}). Absorption spectra (left) and the corresponding absorption difference spectra (right).

12.3 Solvent-Dependent Protonation with TFA in DMSO

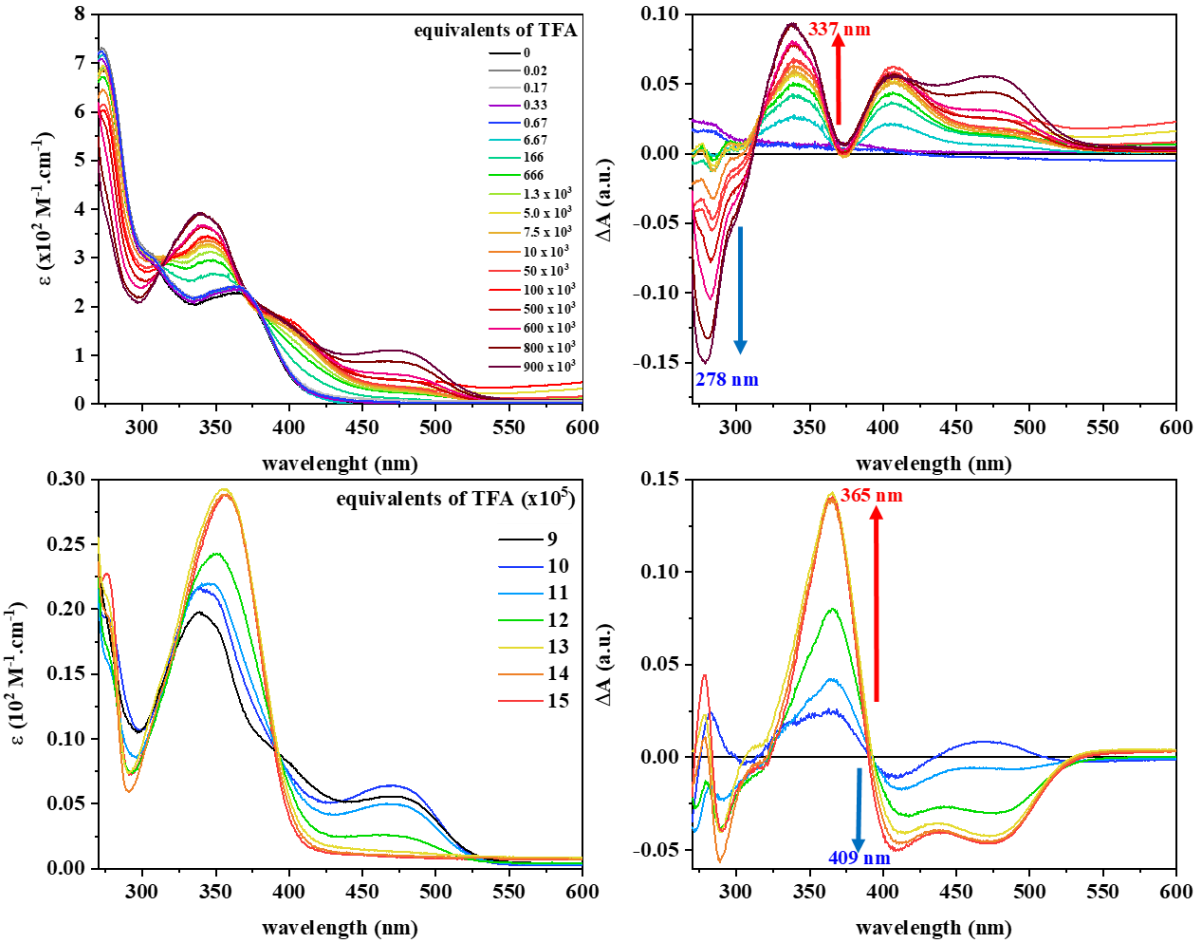

Figure S49. Titration of the model compound **3** with TFA in DMSO ($1.48 \cdot 10^{-5}$ mol·L^{-1}). Absorption spectra (left) and the corresponding absorption difference spectra (right).

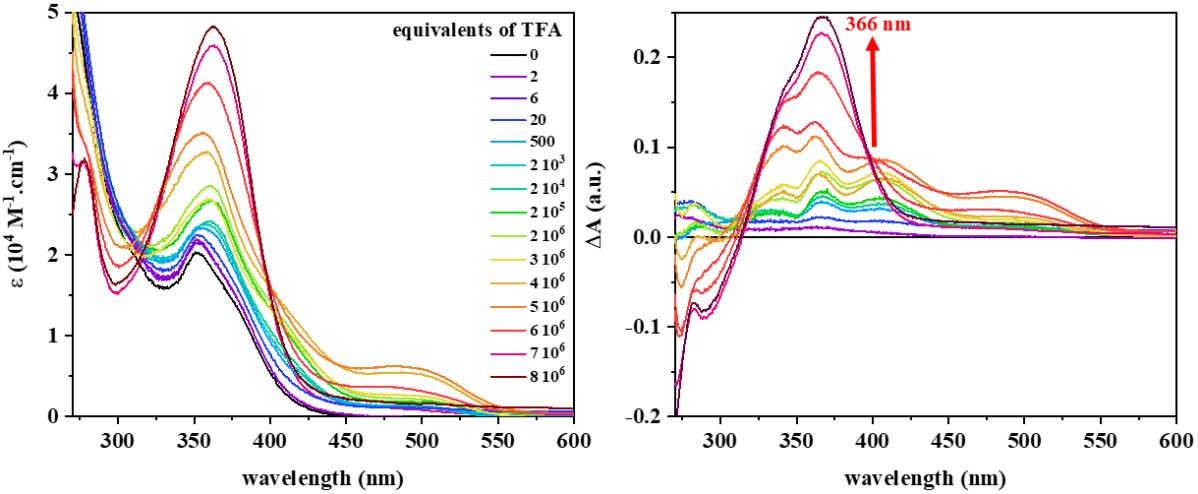

Figure S50. Titration of the cage compound **2** with TFA in DMSO ($1.48 \cdot 10^{-5}$ mol·L^{-1}). Absorption spectra (left) and the corresponding absorption difference spectra (right).

12.4 Emission Spectra

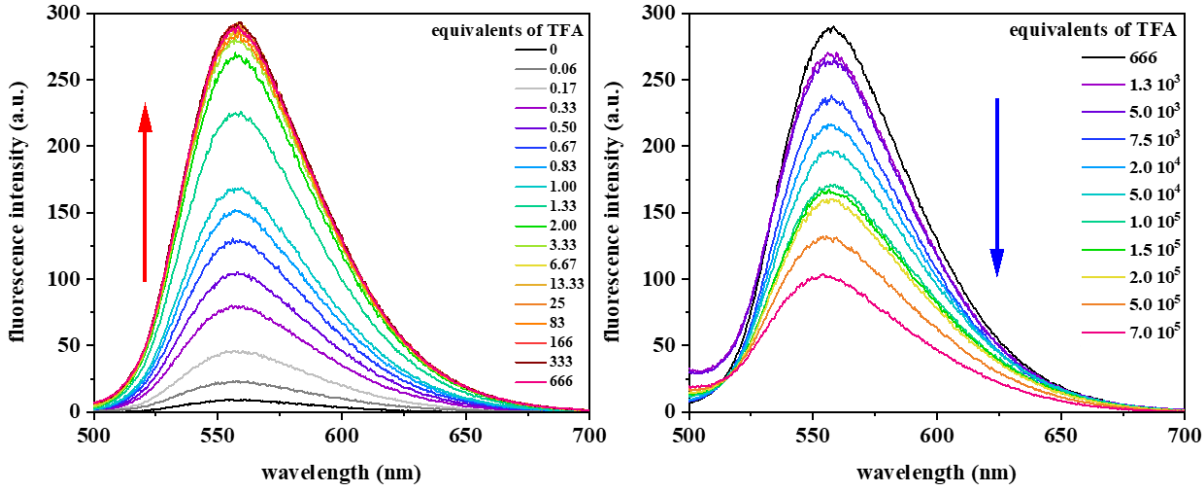

Figure S51. Emission (λ_{ex}=354 nm, λ_{em}=559 nm) spectra of the model compound **3** ($1.48 \cdot 10^{-5}$ mol·L^{-1}) measured in DCM. On the left side, an increase of the emission is observed with increase of the amount of TFA. On the right side, a decrease of the emission is observed with increase of TFA concentration.

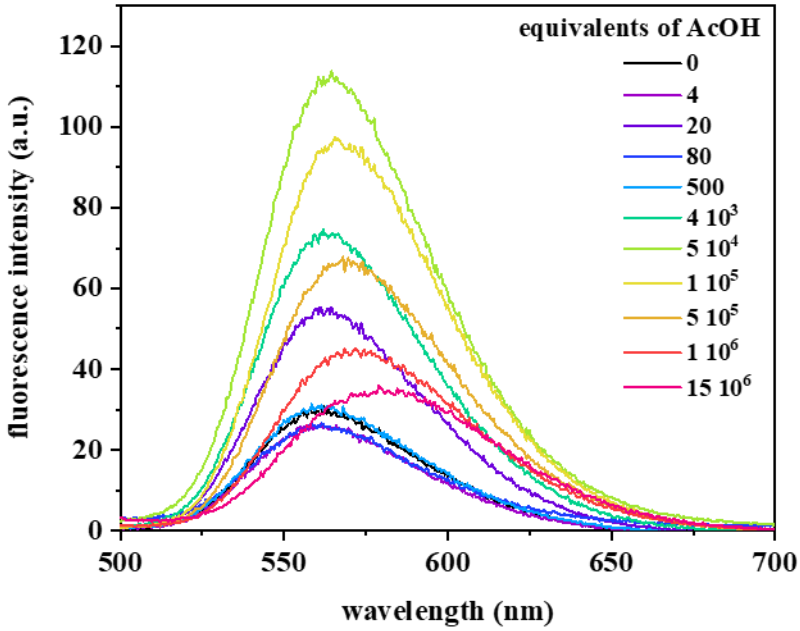

Figure S52. Emission (λ_{ex}=354 nm, λ_{em}=565 nm) spectra of the cage compound **2** ($2.76 \cdot 10^{-6}$ mol·L^{-1}) measured in DCM. A maximum of emission is observed for 4 10^3 equiv. AcOH.

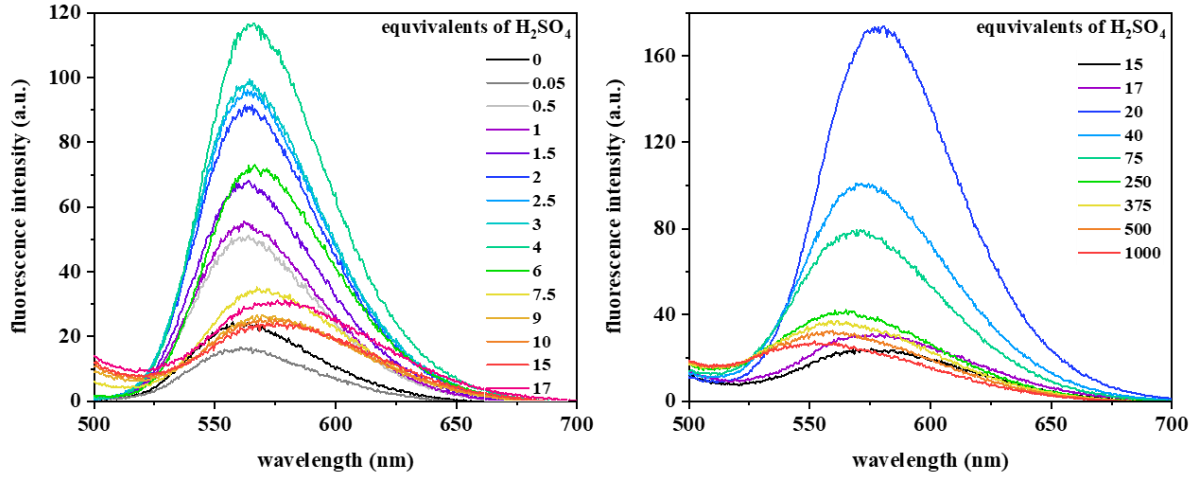

Figure S53. Emission (λ_{ex}=354 nm, λ_{em1}=566 nm, λ_{em2}=577 nm) spectra of the cage compound **2** ($2.76 \cdot 10^{-6}$ mol·L^{-1}) measured in DCM. On the left side, a maximum of emission is observed for 4 equiv. of H_2SO_4. On the left right, a maximum of emission is observed for 20 equiv. of H_2SO_4.

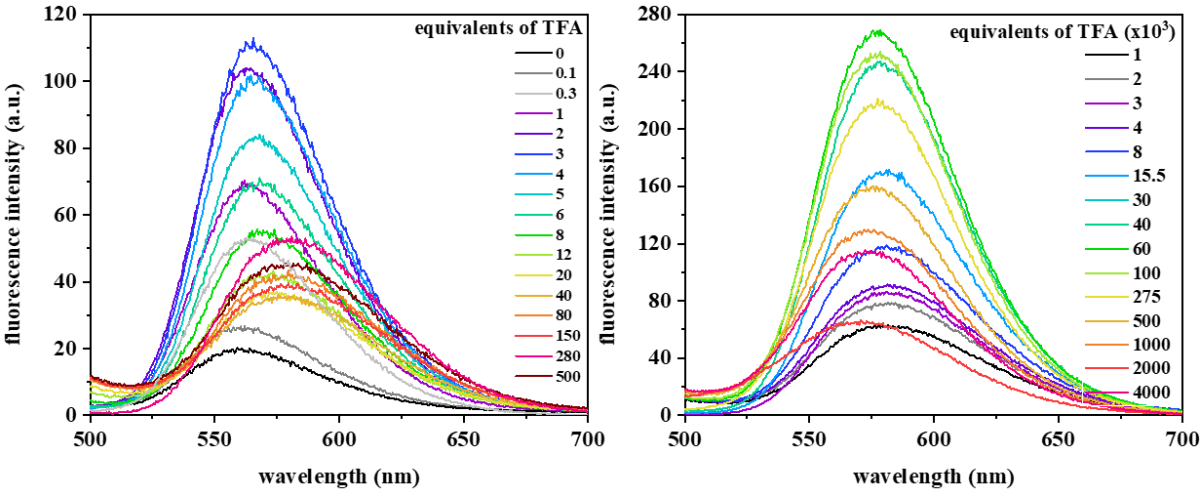

Figure S54. Emission (λ_{ex}=354 nm, λ_{em}=565 nm, λ_{em}=575 nm) spectra of the cage compound **2** ($2.76 \cdot 10^{-6}$ mol·L^{-1}) measured in DCM. On the left side, a maximum of emission is observed for 3 equiv. of TFA. On the left right, a maximum of emission is observed for $40 \cdot 10^3$ equiv. of TFA.

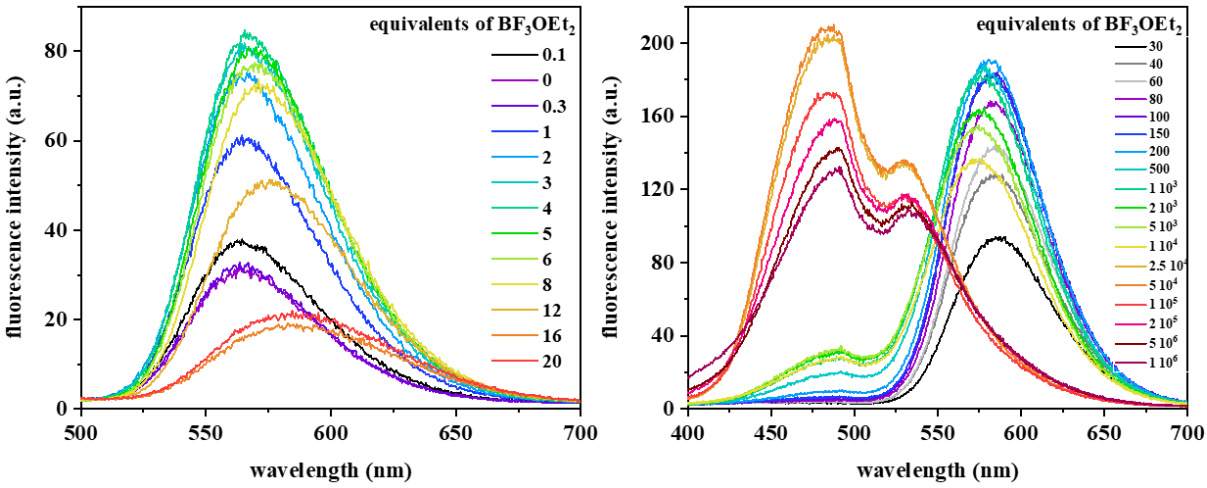

Figure S55. Emission (λ_{ex}=354 nm, λ_{em1}=566 nm, λ_{em2}=580 nm, λ_{em3}=483 nm) spectra of the cage compound **2** ($2.76 \cdot 10^{-6}$ mol·L^{-1}) measured in DCM. On the left side, a maximum of emission is observed for 3 equiv. of $BF_3 \cdot OEt_2$. On the left right, two maximum of emission are observed, one for 200 equiv. of $BF_3 \cdot OEt_2$ and one for 5 10^4 equiv. of $BF_3 \cdot OEt_2$.

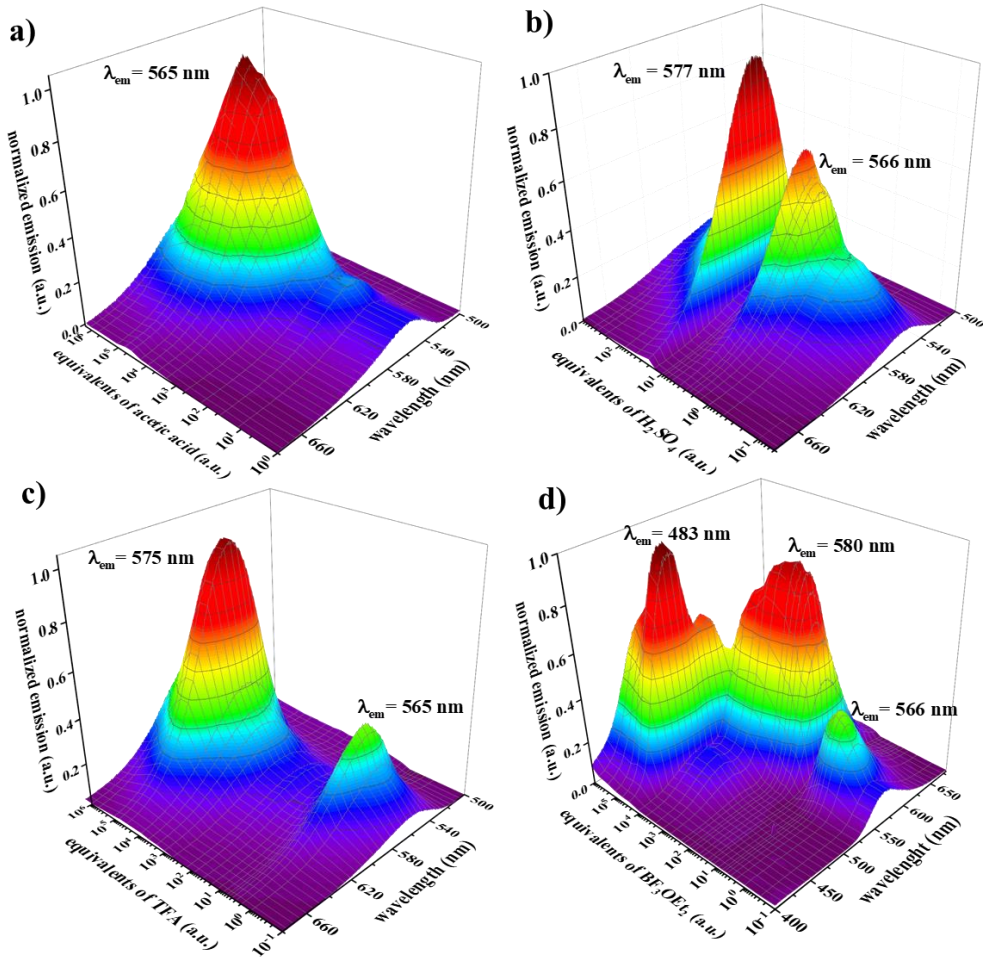

Figure S56. Normalized emission (λ_{ex}=354 nm) of cage compound **2** as 3D-plot measured in DCM for different equivalents of acids. a) AcOH, b) H_2SO_4, c) TFA, d) $BF_3 \cdot OEt_2$. A quantum yield of 6.4% was measured for the cage with $40 \cdot 10^3$ eq of TFA in DCM.

13. Acid Sensing and Reversibility

In solution: To a solution of cage compound **2** (2 mL, $2.76 \cdot 10^{-6}$ mol·L^{-1}) was successively added four equivalents of TFA (8.8 µL, $7.09 \cdot 10^{-2}$ mol·L^{-1}) and four equivalents of TEA (10 µL, $2.23 \cdot 10^{3}$ mol·L^{-1}). This process was repeated nine times; in each case the fluorescence of the solution was measured.

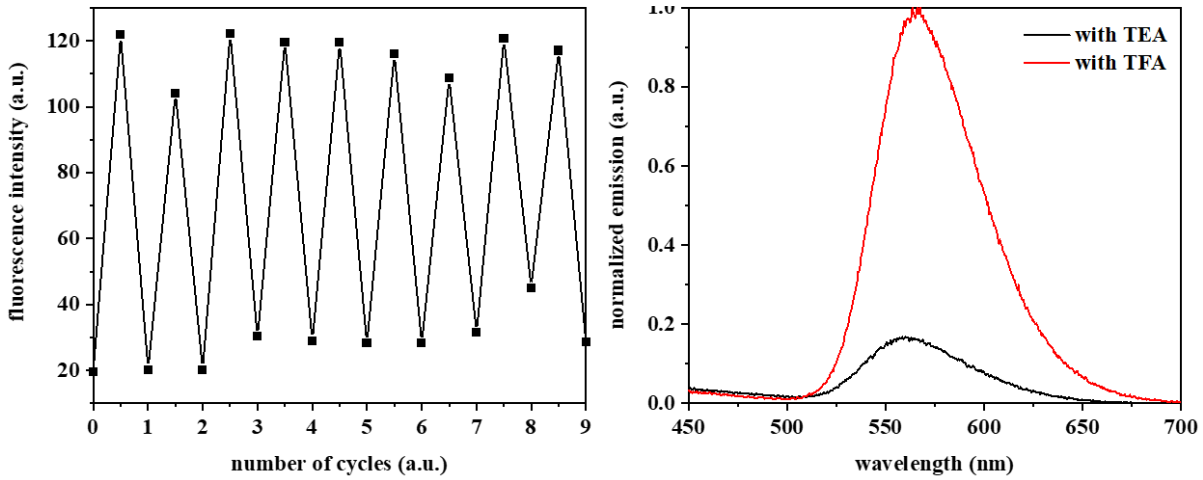

Figure S57. Emission spectrum (right) and reversibility cycles (left) of cage compound **2** in presence of TFA or TEA measured in dichloromethane at room temperature. (C_{Cage} = $2.76 \cdot 10^{-6}$ mol·L^{-1}). This experiment shows the sensibility of the cage to acid, 2.52 µg of TFA was detected.

As thin-films: A thin film of the cage compound **2** was obtained by drop casting few drops of a dioxane solution (~0.2 mg·mL^{-1}) on a microscope slide and slowly evaporated at ambient temperature. The thin-film decorated slide was alternating hold over an open glass with concentrated hydrochloric acid and aqueous ammonia to switch between fluorescence.

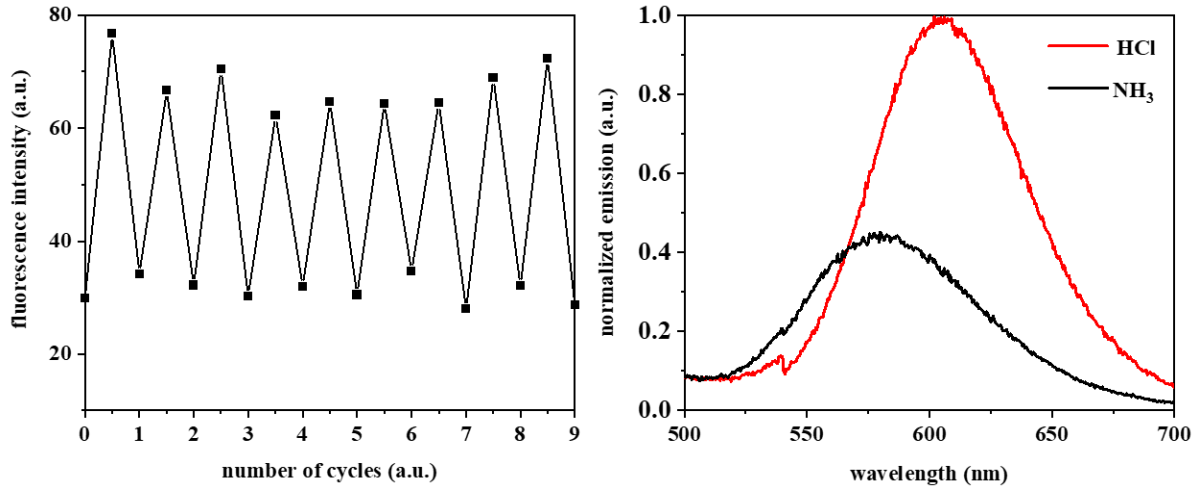

Figure S58. Emission spectrum (right) and reversibility cycles (left) of a thin film of cage compound **2** fumed with HCl and NH_3.

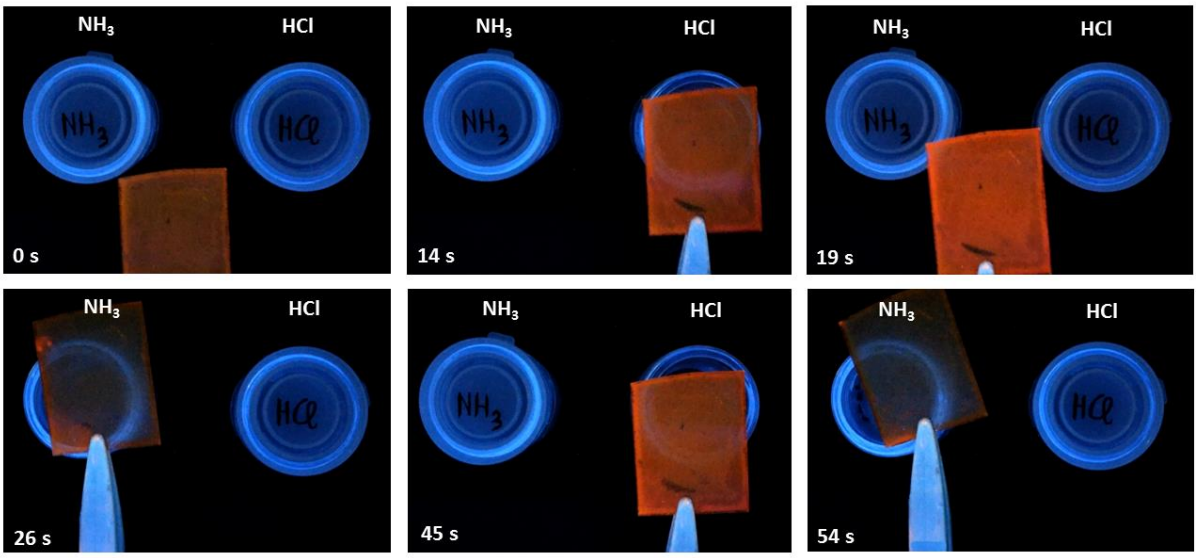

Figure S59. Pictures of cage compound **2** as a thin films showing the fluorescence change under UV-light (254 nm).

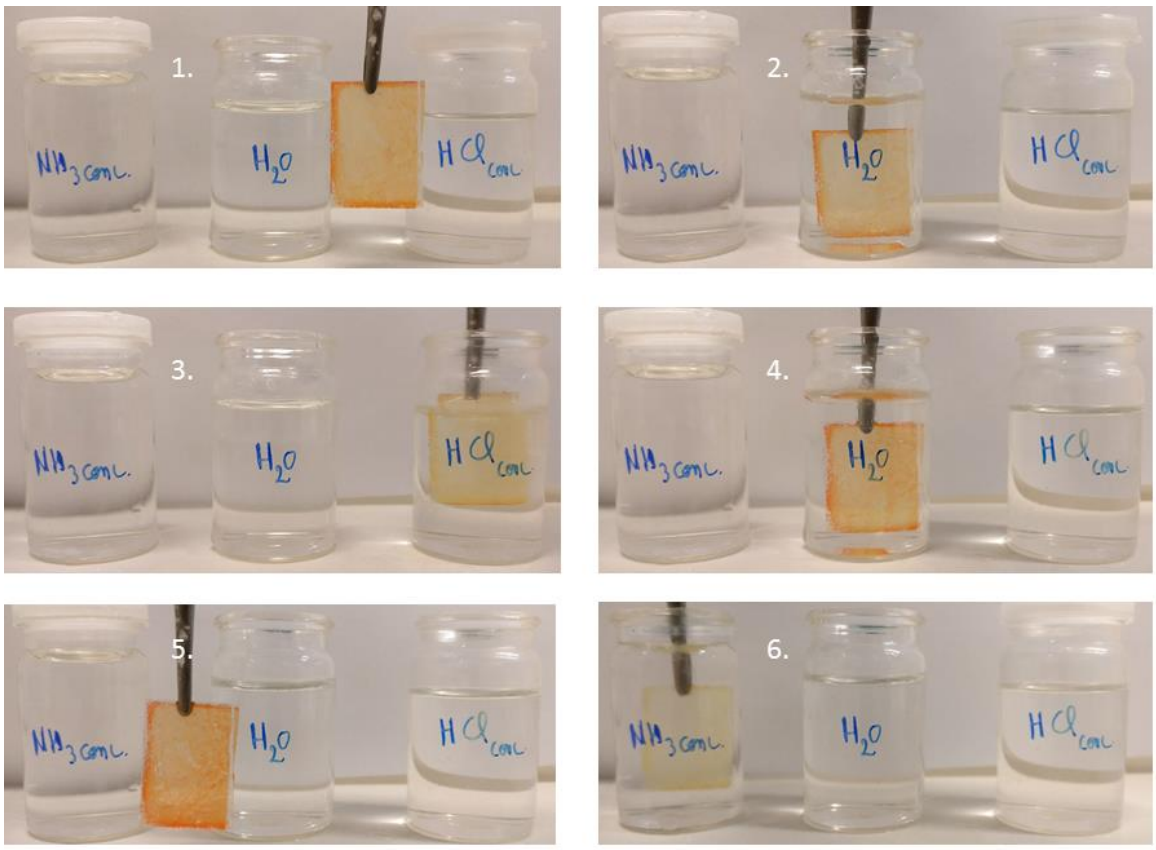

Figure S60. Pictures of cage compound **2** as thin films to demonstrate the chemical stability, when dipped into concentrated hydrochloric acid solution or concentrated ammonia solution.

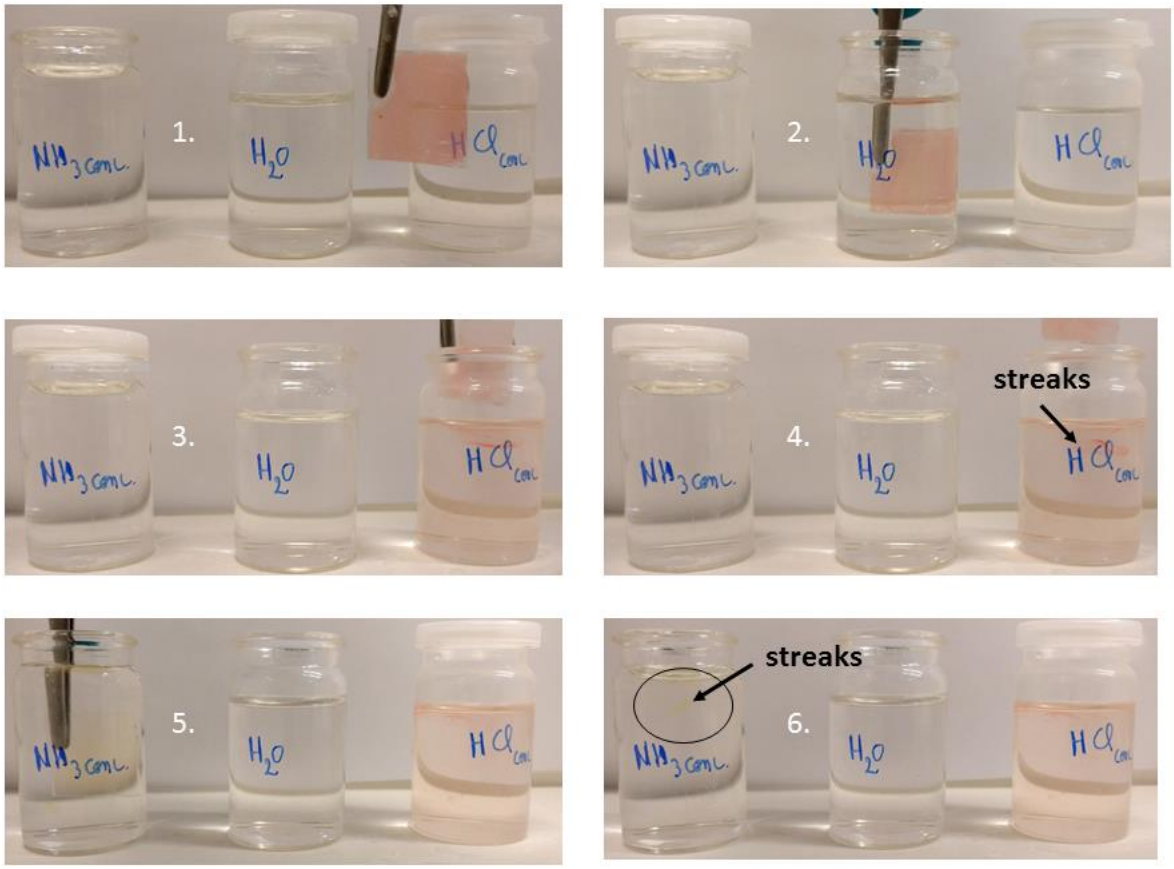

Figure S61. Pictures of cage compound **1** as a thin films to demonstrate the lack of stability, when dipped into concentrated hydrochloric acid solution or concentrated ammonia solution. As soon as the film enters one of the solutions it gets dissolved.

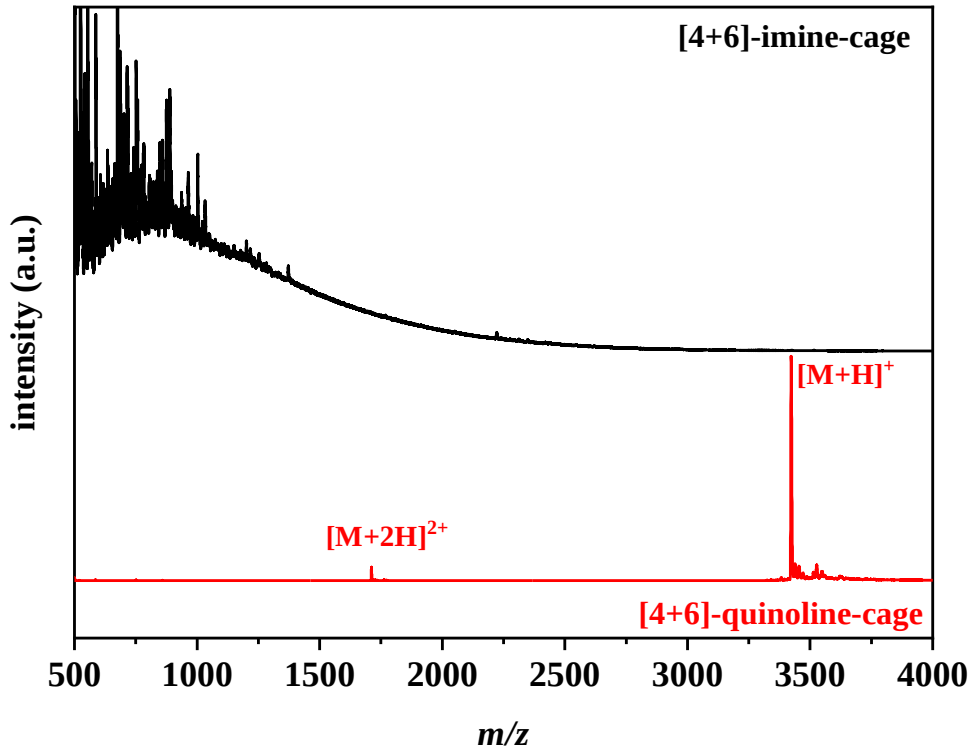

Figure S62. MALDI-TOF (DCBT) spectra of the films after immersion in HCl and NH_3 solutions for imine cage compound **1** (black) and quinoline cage compound **2** (red).

14. Adsorption of $HCl_{(g)}$

In a crucible was placed the cage compound **2** (7 mg). This crucible was placed in a closed-vial with $HCl_{(aq.)}$ (2 mL, 37%).

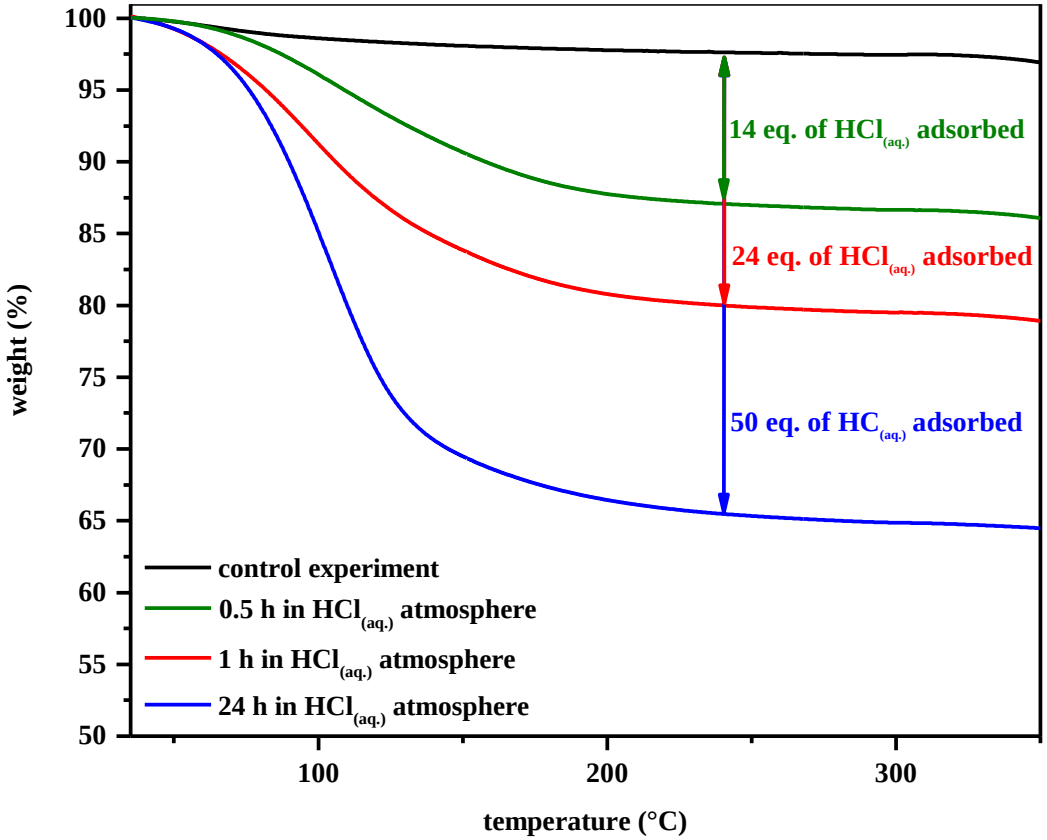

Figure S63. Thermogravimetric analysis of the cage compound **2** (N_2, heating rate: 10 °C/min).

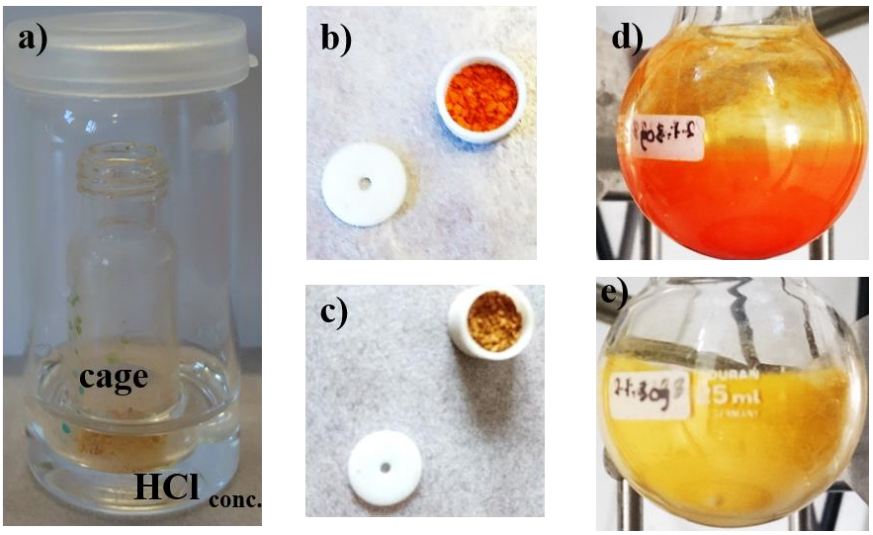

Figure S64. a) Photo of the cage compound **2** placed in a vial under HCl atmosphere. b) Solid of the cage in a crucible as HCl fumed and c) after the TGA measurements (heat regen).d) Solid of the cage in a flask after an acid work-up and. e) same flask after drying at 250 °C and 10^{-3} mbar.

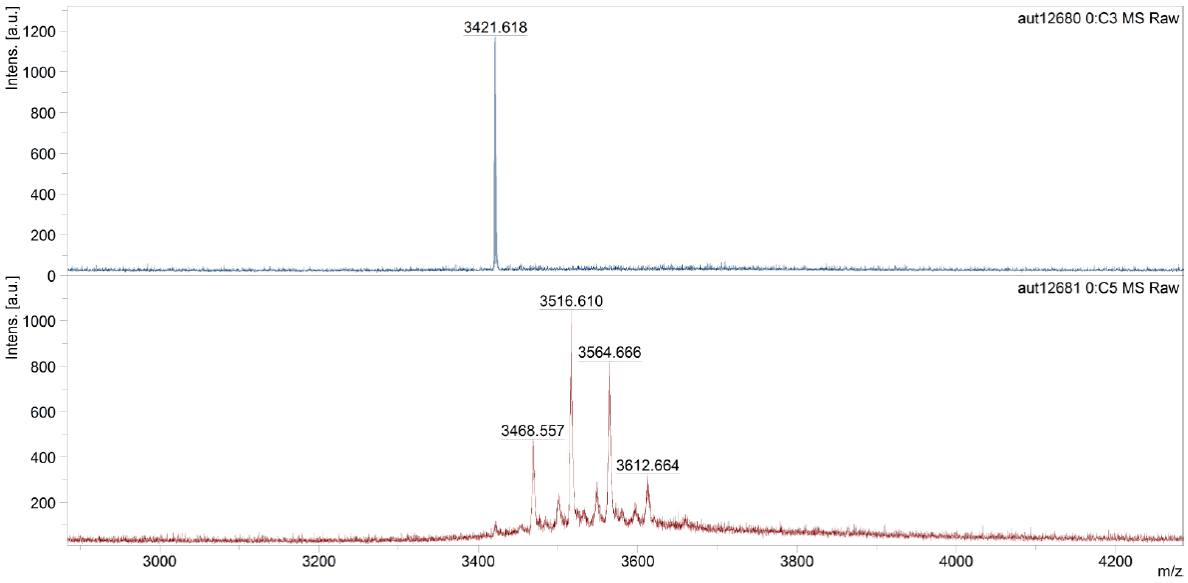

Figure S65. MALDI-TOF comparison (linear mode) of cage **2** and the mixture of cage **2** and $BF_3{\cdot}OEt_2$ in dichloromethane. Matrix: DCTB. The incorporation of up to four "BF_2"-units can be detected.

15. References

[S1] M. Sanz, T. Cuenca, M. Galakhov, A. Grassi, R. K. J. Bott, D. L. Hughes, S. J. Lancaster, M. Bochmann, *Organometallics* **2004**, *23*, 5324-5331.

[S2] A. S. Bhat, S. M. Elbert, W.-S. Zhang, F. Rominger, M. Dieckmann, R. R. Schröder, M. Mastalerz, *Angew. Chem. Int. Ed.* **2019**, *58*, 8819-8823.

[S3] S. Viel, F. Ziarelli, G. Pagès, C. Carrara, S. Caldarelli, *J. Magn. Reson.* **2008**, *190*, 113-123.

[S4] aA. Gierer, K. Wirtz, in *Zeitschrift für Naturforschung A, Vol. 8*, **1953**, p. 532; bH. C. Chen, S. H. Chen, *The Journal of Physical Chemistry* **1984**, *88*, 5118-5121.

[S5] Y. H. Zhao, M. H. Abraham, A. M. Zissimos, *The Journal of Organic Chemistry* **2003**, *68*, 7368-7373.

[S6] C. Würth, M. Grabolle, J. Pauli, M. Spieles, U. Resch-Genger, *Nature Protocols* **2013**, *8*, 1535-1550.